

RECEIVED: February 27, 2017

REVISED: August 13, 2017

ACCEPTED: August 29, 2017

PUBLISHED: September 25, 2017

Top-quark mass measurement in the all-hadronic $t\bar{t}$ decay channel at $\sqrt{s} = 8$ TeV with the ATLAS detector



The ATLAS collaboration

E-mail: atlas.publications@cern.ch

ABSTRACT: The top-quark mass is measured in the all-hadronic top-antitop quark decay channel using proton-proton collisions at a centre-of-mass energy of $\sqrt{s} = 8$ TeV with the ATLAS detector at the CERN Large Hadron Collider. The data set used in the analysis corresponds to an integrated luminosity of 20.2 fb^{-1} . The large multi-jet background is modelled using a data-driven method. The top-quark mass is obtained from template fits to the ratio of the three-jet to the dijet mass. The three-jet mass is obtained from the three jets assigned to the top quark decay. From these three jets the dijet mass is obtained using the two jets assigned to the W boson decay. The top-quark mass is measured to be 173.72 ± 0.55 (stat.) ± 1.01 (syst.) GeV.

KEYWORDS: Hadron-Hadron scattering (experiments), Top physics

ARXIV EPRINT: [1702.07546](https://arxiv.org/abs/1702.07546)

Contents

1	Introduction	1
2	ATLAS detector	3
3	Data and Monte Carlo simulation	3
4	Event selection	4
5	$t\bar{t}$ reconstruction	6
6	Multi-jet background estimation	6
7	Top-quark mass determination	8
8	Method validation and template closure	11
9	Systematic uncertainties	13
9.1	Theory and modelling uncertainties	13
9.2	Method-dependent uncertainties	15
9.3	Calibration- and detector-related uncertainties	17
10	Measurement of m_{top}	18
11	Conclusion	19
	The ATLAS collaboration	24

1 Introduction

Of all known fundamental particles, the top quark has the largest mass. Its existence was predicted in 1973 by Kobayashi and Maskawa [1], and it was not observed directly until 1995, by the CDF and D0 experiments at the Tevatron [2, 3]. Since 2010, top quarks have also been observed at the Large Hadron Collider (LHC) [4] at CERN. Due to the higher centre-of-mass energy, top quark production at the LHC is an order of magnitude larger than at the Tevatron. The large data sets of top-antitop quark ($t\bar{t}$) pairs allow many precision studies and measurements of top quark properties. The Yukawa coupling of the top quark is predicted to be close to unity [5, 6], suggesting that it may play a special role in electroweak symmetry breaking. In the Standard Model (SM), the top quark dominantly contributes to the quantum corrections to the Higgs self coupling [7, 8]. Precise measurements of the top-quark mass (m_{top}) are therefore very important in probing the stability of the vacuum [9, 10], and contribute to searches for signs of physics beyond the SM.

Today the most precise individual measurement of m_{top} is in the single-lepton decay channel of top-antitop quark pairs, where one top quark decays into a b -quark, a charged lepton and a neutrino and the other top quark decays into a b -quark and two $u/d/c/s$ -quarks, performed by the CMS Collaboration, yielding a value of $m_{\text{top}} = 172.35 \pm 0.16$ (stat.) ± 0.48 (syst.) GeV [11]. The most precise measurement of m_{top} in the dileptonic $t\bar{t}$ decay channel, where each of the top quarks decays into a b -quark, a charged lepton and its neutrino, is from the ATLAS Collaboration, yielding a value of $m_{\text{top}} = 172.99 \pm 0.41$ (stat.) ± 0.74 (syst.) GeV [12]. Further m_{top} results are available in refs. [13–15].

The top-quark mass measurement in the all-hadronic $t\bar{t}$ channel takes advantage of the largest branching ratio (46%) among the possible top quark decay channels [16]. The all-hadronic channel involves six jets at leading order, two originating from b -quarks and four originating from the two W boson hadronic decays. It is a challenging measurement because of the large multi-jet background arising from various quantum chromodynamics (QCD) processes, which can exceed the $t\bar{t}$ production by several orders of magnitude. However, all-hadronic $t\bar{t}$ events profit from having no neutrinos among the decay products, so that all four-momenta can be measured directly. The multi-jet background for the all-hadronic $t\bar{t}$ channel, while large, leads to different systematic uncertainties than in the case of the single- and dileptonic $t\bar{t}$ channels. Thus, all-hadronic analyses offer an opportunity to cross-check top-quark mass measurements performed in the other channels. The most recent measurements of m_{top} in the all-hadronic channel were performed by the CMS Collaboration with $m_{\text{top}} = 172.32 \pm 0.25$ (stat.) ± 0.59 (syst.) GeV [11], and the ATLAS Collaboration with $m_{\text{top}} = 175.1 \pm 1.4$ (stat.) ± 1.2 (syst.) GeV [17].

This paper presents a top-quark mass measurement in the $t\bar{t}$ all-hadronic channel using data collected by the ATLAS experiment in 2012. The m_{top} measurement is obtained from template fits to the distribution of the ratio of three-jet to dijet masses ($R_{3/2} = m_{jjj}/m_{jj}$), similarly to a previous measurement at $\sqrt{s} = 7$ TeV [17]. The three-jet mass is obtained from the three jets assigned to the top quark decay. From the selected three jets the dijet mass is obtained using the two jets assigned to the W boson decay. The jet assignment is accomplished by using a χ^2 fit to the $t\bar{t}$ system, so there are two values of $R_{3/2}$ measured in each event. The observable $R_{3/2}$ employed in this analysis achieves a partial cancellation of systematic effects common to the masses of the reconstructed top quark and associated W boson, notably the significant uncertainty on the jet energy scale. Data-driven techniques are used to estimate the contribution from multi-jet background events. Data events are divided into several disjoint regions using two uncorrelated observables. The region containing the largest relative fraction of $t\bar{t}$ events is labeled the signal region. The background is estimated from the other regions, which determine the shape of the background distribution in the signal region.

The paper is organised as follows. After a brief description of the ATLAS detector in section 2, the data and Monte Carlo (MC) samples used in the analysis are described in section 3. The analysis event selection is further detailed in section 4. Section 5 describes the method used to select the candidate four-momenta that comprise the reconstructed $t\bar{t}$ system. The estimation of the multi-jet background is detailed in section 6. The method

used to measure the top-quark mass and its uncertainties are reported in sections 7, 8, and 9. The results of the measurement are presented in section 10, and the analysis is summarised in section 11.

2 ATLAS detector

The ATLAS detector [18] is a multi-purpose particle physics experiment with a forward-backward symmetric cylindrical geometry and near 4π coverage in solid angle.¹ The inner tracking detector (ID) covers the pseudorapidity range $|\eta| < 2.5$, and consists of a silicon pixel detector, a silicon microstrip detector, and, for $|\eta| < 2.0$, a transition radiation tracker. The ID is surrounded by a thin superconducting solenoid providing a 2 T magnetic field. A high-granularity lead/liquid-argon (LAr) sampling electromagnetic calorimeter covers the region $|\eta| < 3.2$. A steel/scintillator-tile calorimeter provides hadronic coverage in the range $|\eta| < 1.7$. LAr technology is also used for the hadronic calorimeters in the endcap region $1.5 < |\eta| < 3.2$ and for electromagnetic and hadronic measurements in the forward region up to $|\eta| = 4.9$. The muon spectrometer surrounds the calorimeters. It consists of three large air-core superconducting toroid systems, precision tracking chambers providing accurate muon tracking for $|\eta| < 2.7$, and additional detectors for triggering in the region $|\eta| < 2.4$.

3 Data and Monte Carlo simulation

This analysis is performed using the proton-proton (pp) collision data set at a centre-of-mass energy of $\sqrt{s} = 8$ TeV collected with the ATLAS detector at the LHC. The data correspond to an integrated luminosity of 20.2 fb^{-1} . Samples of simulated MC events are used to optimise the analysis, to study the detector response and the efficiency to reconstruct $t\bar{t}$ events, to build signal template distributions used for fitting the top-quark mass, and to estimate systematic uncertainties. Most of the MC samples used in the analysis are based on a full simulation of the ATLAS detector [19] obtained using GEANT4 [20]. Some of the systematic uncertainties are studied using alternative $t\bar{t}$ samples processed through a faster ATLAS simulation (AFII) using parameterised showers in the calorimeters [21]. Additional simulated pp collisions generated with PYTHIA [22] are overlaid to model the effects of additional collisions in the same and nearby bunch crossings (pile-up). All simulated events are processed using the same reconstruction algorithms and analysis chain as used for the data.

The nominal $t\bar{t}$ simulation sample is generated using the next-to-leading-order (NLO) MC program POWHEG-BOX [23–25] with the NLO parton distribution function (PDF) set CT10 [26, 27], interfaced to PYTHIA 6.427 [28] with a set of tuned parameters called

¹The coordinate system used to describe the ATLAS detector is briefly summarised here. The nominal interaction point is defined as the origin of the coordinate system, while the beam direction defines the z -axis and the x - y plane is transverse to the beam direction. The positive x -axis is defined as pointing from the interaction point to the centre of the LHC ring and the positive y -axis is defined as pointing upwards. The azimuthal angle ϕ is measured around the beam axis, and the polar angle θ is the angle from the beam axis. The pseudorapidity is defined as $\eta = -\ln \tan(\theta/2)$. The transverse momentum p_T , the transverse energy E_T , and the missing transverse momentum (E_T^{miss}) are defined in the x - y plane unless stated otherwise. The distance ΔR in the η - ϕ angle space is defined as $\Delta R = \sqrt{(\Delta\eta)^2 + (\Delta\phi)^2}$.

the PERUGIA 2012 tune [29] for parton shower, fragmentation and underlying-event modelling. For the construction of the signal templates, MC events are generated at five different assumed values of m_{top} , between 167.5 and 177.5 GeV, in steps of 2.5 GeV. The full simulation of the ATLAS detector sample at 172.5 GeV has the largest number of generated events, and is used as the nominal signal sample. The h_{damp} parameter [30], which regulates the high- p_{T} radiation in POWHEG-BOX, is set to the same m_{top} value as used in each of the generated POWHEG-BOX samples. All the simulated samples used to estimate systematic uncertainties are further described in section 9.

All MC samples are normalised using the predicted top-antitop quark pair cross-section ($\sigma_{t\bar{t}}$) at $\sqrt{s} = 8$ TeV. For $m_{\text{top}} = 172.5$ GeV, the next-to-next-to-leading-order cross-section of $\sigma_{t\bar{t}} = 253_{-15}^{+13}$ pb is calculated using the program TOP++2.0 [31], which includes re-summation of next-to-next-to-leading logarithmic soft gluon terms.

4 Event selection

Events in this analysis are selected by a trigger that requires at least five jets with $p_{\text{T}} > 55$ GeV. Only events with a well-reconstructed primary vertex formed by at least five tracks with $p_{\text{T}} > 400$ MeV are considered for the analysis. Events with isolated electrons (muons) with $E_{\text{T}} > 25$ GeV ($p_{\text{T}} > 20$ GeV) and reconstructed in the central region of the detector within $|\eta| < 2.5$ are rejected. Both lepton types are identified using the tight working points as specified in refs. [32, 33]. Jets (j) are reconstructed using the anti- k_{t} algorithm with radius parameter $R = 0.4$ [34] employing topological clusters [35] in the calorimeter. These jets are calibrated to the hadronic energy scale as described in refs. [36–38]. The four-vector of the highest-energy muon (μ) from among those matched within $\Delta R(j, \mu) < 0.3$ to a reconstructed jet, is added to the reconstructed jet four-vector. This is done to compensate for the energy losses in the calorimeter arising from semimuonic quark decays. In simulation this correction slightly improves both the jet energy response and resolution across the full range of jet energies.

To ensure that the selected events are in the plateau region of the trigger efficiency curve where the trigger efficiency in data is greater than 90%, at least five of the reconstructed central jets (within $|\eta| < 2.5$) are required to have $p_{\text{T}} > 60$ GeV. Any additional jet is required to have $p_{\text{T}} > 25$ GeV and $|\eta| < 2.5$. All selected jets in an event must be isolated; any pairing of two jets (j_i and j_k) reconstructed with the above criteria are required to not overlap within $\Delta R(j_i, j_k) < 0.6$. Events with jets failing this isolation requirement are rejected.

Events containing neutrinos are removed by requiring $E_{\text{T}}^{\text{miss}} < 60$ GeV. The $E_{\text{T}}^{\text{miss}}$ in an event is computed as the sum of a number of different terms [39, 40]. Muons, electrons and jets are accounted for using the appropriate calibrations for each object. For each term considered, the missing transverse momentum is calculated as the negative sum of the calibrated reconstructed objects, projected onto the x and y directions.

For the final selection, events are kept if at least two of the six leading transverse momentum jets are identified as originating from a b -quark. Such jets are said to be b -tagged. A neural network trained on decay vertex properties [41] is used to identify these b -tagged jets. Because of the large number of c -quarks originating from the W boson

Cut	Event yields (thousands)	
	Data	$t\bar{t}$ all-hadronic (MC)
Initial	850450	2338 ± 1
$N_{\text{PV}>4 \text{ tracks}}$ & no isolated e/μ	33476	308.7 ± 0.6
Trigger: 5 jets with $p_{\text{T}} > 55 \text{ GeV}$ & ≥ 6 good jets	16110	241.4 ± 0.5
No 2 good jets (j_i, j_k) within $\Delta R(j_i, j_k) < 0.6$	7646	142.9 ± 0.4
≥ 5 good jets with $p_{\text{T}} > 60 \text{ GeV}$	3303	51.4 ± 0.2
$E_{\text{T}}^{\text{miss}} < 60 \text{ GeV}$	3021	46.3 ± 0.2
$\Delta\phi(b_i, b_j) > 1.5$	1737	30.9 ± 0.2
$\chi^2 < 11$	645.8	22.3 ± 0.1
$N_{b_{\text{tag}}} \geq 2$	21.9	6.61 ± 0.08
$\langle \Delta\phi(b, W) \rangle < 2$	12.9	4.40 ± 0.07

Table 1. Event yields following each of the individual event selection cuts, with values shown for both the data and all-hadronic MC events generated at $m_{\text{top}} = 172.5 \text{ GeV}$ (shown with statistical uncertainty). The $t\bar{t}$ contribution is after scaling to the theoretical cross-section and integrated luminosity. $N_{\text{PV}>4 \text{ tracks}}$ is the number of primary vertices with > 4 tracks. Good jets have $p_{\text{T}} > 25 \text{ GeV}$ and $|\eta| < 2.5$.

decays in this analysis (on average one c -quark per $t\bar{t}$ event) a b -tagger trained to reject $u/d/s$ -jets but also a large fraction of c -jets is used. Events with fewer than two b -tagged jets are used for the background estimate described in section 6. The chosen working point for the b -tagging neural network has an identification efficiency of about 57% [42] for jets from b -quarks, with a rejection factor of about 330 for jets arising from $u/d/s$ -quarks, and a factor of about 13 for jets arising from c -quarks.

In each event the two jets with leading b -tag weights (b_i and b_j) are required to satisfy $\Delta\phi(b_i, b_j) > 1.5$. The quantities b_i and b_j represent here the 4-vectors of the i -th and j -th jet. This $\Delta\phi$ cut is very powerful in rejecting combinatorial background events; most of these are true $t\bar{t}$ events where the incorrect jets are associated with the top quark. Finally, a cut is applied based on the azimuthal angle between b -jets and their associated W boson candidate: the average of the two angular separations for each event is required to satisfy $\langle \Delta\phi(b, W) \rangle < 2$. Here the b , and the W are the 4-vectors of a b -jet and a W , identified by means of the three-jet combination that best fits the $t\bar{t}$ event hypothesis described in section 5. This $\Delta\phi$ cut rejects a large fraction of events from the multi-jet and combinatorial backgrounds, as well as events from non-all-hadronic $t\bar{t}$ decays. Events failing this final selection cut are, however retained for the purpose of modelling the multi-jet background, as detailed in section 6.

Table 1 summarises the yields obtained after each of the individual selection cuts. The χ^2 cut listed in table 1 is described in section 5. The number of b -tagged jets ($N_{b_{\text{tag}}}$) and $\langle \Delta\phi(b, W) \rangle$ are the two observables used for the data-driven multi-jet background estimation, further detailed in section 6.

A top quark reconstruction purity of $58.8\% \pm 0.2\%$ is achieved after applying all event selection cuts shown in table 1. This purity is defined as the fraction of the number of correctly reconstructed top quarks relative to the number of the sum of both correctly and incorrectly reconstructed top quarks. It is evaluated in simulation, and based on the matching of reconstructed jets to truth-record quarks from the top quark decays.

5 $t\bar{t}$ reconstruction

In each event the $t\bar{t}$ final state is reconstructed using all the jets from the all-hadronic $t\bar{t}$ decay chain: $t\bar{t} \rightarrow bWbW \rightarrow b_1j_1j_2b_2j_3j_4$. To determine the top-quark mass in each $t\bar{t}$ event, a minimum- χ^2 approach is adopted, with the χ^2 defined as:

$$\chi^2 = \frac{(m_{b_1j_1j_2} - m_{b_2j_3j_4})^2}{\sigma_{\Delta m_{bjj}}^2} + \frac{(m_{j_1j_2} - m_W^{\text{MC}})^2}{\sigma_{m_W^{\text{MC}}}^2} + \frac{(m_{j_3j_4} - m_W^{\text{MC}})^2}{\sigma_{m_W^{\text{MC}}}^2}. \quad (5.1)$$

Here, two of the reconstructed jets are associated with the bottom-type quarks produced directly from the top quark and antitop quark decays (b_1 and b_2), the other four jets are assumed to be $u/d/c/s$ -quark jets from the W boson hadronic decay (j_i , where $i = 1, \dots, 4$), and $\Delta m_{bjj} = m_{b_1j_1j_2} - m_{b_2j_3j_4}$. This method considers all possible permutations of the six or more reconstructed jets in each event. The permutation resulting in the lowest χ^2 value is kept. A low χ^2 value indicates a permutation of jets consistent with the $t\bar{t}$ hypothesis. No explicit b -tagging information is used in eq. (5.1).

In each combination the reconstructed masses of the two hadronically decaying W bosons ($m_{j_1j_2}$ and $m_{j_3j_4}$) in data are compared to the mean of the mass distribution of correctly reconstructed W bosons in simulated signal MC events (m_W^{MC}). The correct reconstruction of the top quarks and the W bosons in a simulated event is achieved by matching parton-level particles to the event's jets. The widths ($\sigma_{m_W^{\text{MC}}}$ and $\sigma_{\Delta m_{bjj}}$) used in the denominators of eq. (5.1) are obtained from fits to a single Gaussian function to the mass distributions of the correctly reconstructed top quarks and W bosons: $\sigma_{\Delta m_{bjj}} = 21.60 \pm 0.16$ (stat.) GeV and $\sigma_{m_W^{\text{MC}}} = 7.89 \pm 0.05$ (stat.) GeV. The m_W^{MC} mean value used in eq. (5.1) is determined to be 81.18 ± 0.04 (stat.) GeV. To reduce the multi-jet background in the analysis and to eliminate events where the top quarks and the W bosons in an event are not reconstructed correctly, a minimum $\chi^2 < 11$ is required.

6 Multi-jet background estimation

The available MC generators for multi-jet production include only leading-order theory calculations for final states with up to six partons. Therefore, the dominant multi-jet background in this analysis is determined directly from the data. Two largely uncorrelated variables are used to divide the data events into four different regions, such that the background is determined in the control regions and extrapolated to the signal region. The two chosen observables are the $N_{b_{\text{tag}}}$ in an event, and the $\langle \Delta\phi(b, W) \rangle$ variable, both described in section 4. These have a linear correlation measured in data of $\rho = -0.038$. The value of $N_{b_{\text{tag}}}$ in each event is determined from the leading six jets ordered by p_T .

ABCD region and definition			Estimated signal fraction
Region	$N_{b_{\text{tag}}}$	$\langle \Delta\phi(b, W) \rangle$	$t\bar{t}$ MC/data [%]
A	< 2	≥ 2.0	2.06 ± 0.02
B	< 2	< 2.0	2.60 ± 0.02
C	≥ 2	≥ 2.0	24.71 ± 0.55
D	≥ 2	< 2.0	34.05 ± 0.57

Table 2. Definitions and signal fractions for each of the four regions used to estimate the multi-jet background. Region D is the signal region. The signal fraction with statistical uncertainty is estimated by comparing the total predicted number of signal events from $t\bar{t}$ simulation to the number of observed data events in each region.

The four regions, labelled ABCD, are identified by defining two bins in the number of b -tagged jets, $N_{b_{\text{tag}}} < 2$, $N_{b_{\text{tag}}} \geq 2$, and two ranges of the $\langle \Delta\phi(b, W) \rangle$ variable, $\langle \Delta\phi(b, W) \rangle < 2.0$, $\langle \Delta\phi(b, W) \rangle \geq 2.0$, as detailed in table 2. The $R_{3/2}$ distributions are studied for each of the defined regions. Region D represents the signal region (SR), and contains the largest fraction of $t\bar{t}$ events (34.05%). Regions A, B, and C are the control regions (CR), and are dominated by multi-jet background events. Table 2 summarises the expected fractions of signal events in each of the four regions. Each signal fraction is estimated by comparing the total predicted number of signal events from $t\bar{t}$ simulation to the number of observed data events in each region.

To obtain an unbiased estimate of the number of background events in each considered CR, the signal contamination is removed using simulated $t\bar{t}$ events with $m_{\text{top}} = 172.5$ GeV. The method validation and the template closure described in section 8 show that the m_{top} dependence of this signal subtraction is significantly smaller than other uncertainties on the method, and is ignored. The estimated background in a given bin i of $R_{3/2}$ for SR D ($N_{\text{background},i}^{\text{SR D}}$) is given by:

$$N_{\text{background},i}^{\text{SR D}} = \left(\frac{N_{\text{background}}^{\text{CR C}}}{N_{\text{background}}^{\text{CR A}}} \right) N_{\text{background},i}^{\text{CR B}}. \tag{6.1}$$

This corresponds to the background in a given bin i of the $R_{3/2}$ spectrum of CR B ($N_{\text{background},i}^{\text{CR B}}$), estimated after subtraction of the signal contamination, and scaled by the ratio of the number of events in control regions C ($N_{\text{background}}^{\text{CR C}}$) and A ($N_{\text{background}}^{\text{CR A}}$), also after signal removal. The signal contamination present in CR C comes from improperly reconstructed $t\bar{t}$ events which form a smoothly varying distribution in $R_{3/2}$. This signal contribution in CR C is not relevant in the analysis, as this region only affects the normalisation of the distribution obtained for the multi-jet background, which is not used in the fit for m_{top} described in section 7.

Figure 1 shows the distributions of the masses of the W boson (m_{jj}) and top quark (m_{jjj}) after applying the event selection, the χ^2 approach defined in eq. (5.1), and using the data-driven multi-jet background method. In the figure, the reconstruction using MC events is said to be correct for one (or both) top quark(s) if each of the three jets (j)

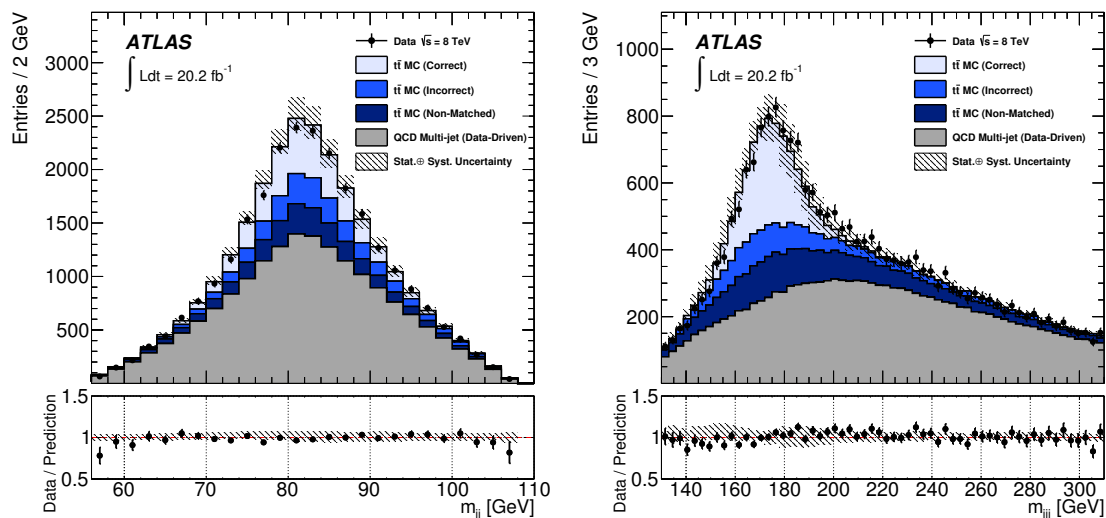


Figure 1. Dijet invariant mass distribution, m_{jj} , for W boson candidates (left) and three-jet invariant mass, m_{jjj} , for top quark candidates (right) in data compared to the sum of $t\bar{t}$ simulation and multi-jet background. The ratio comparing data to prediction is shown below each distribution. The hatched bands reflect the sum of the statistical and systematic errors added in quadrature. The $t\bar{t}$ simulation corresponds to $m_{\text{top}} = 172.5$ GeV.

selected by the reconstruction algorithm matches to each of the three quarks (q) within a $\Delta R(j, q) < 0.3$, modulo the interchange of the two jets assigned to the hadronically decaying W boson. If at least one of the jets selected by the algorithm is not one of the three jets matched to the quarks, the top quark reconstruction is classified as incorrect. Finally, cases where at least one quark is not matched uniquely to a reconstructed jet are classified as non-matched. The $R_{3/2}$ distribution obtained after using the data-driven multi-jet background estimation methods to determine the shape and normalisation is shown in figure 2. In general, good agreement between data and prediction is observed in all the distributions.

7 Top-quark mass determination

To extract a measurement of the top-quark mass, a template method with a binned minimum- χ^2 approach is employed. For each $t\bar{t}$ event, two $R_{3/2}$ values are obtained, one for each top-quark mass measurement. To properly correct for the linear correlation between the two $R_{3/2}$ values in each event, the statistical uncertainty of m_{top} returned from the final χ^2 fit described later in this section is scaled up by a factor $\sqrt{1 + \rho} = 1.26$, where $\rho = 0.59$ is the correlation factor as obtained from data. Signal and background templates binned in $R_{3/2}$ are created using the simulated $t\bar{t}$ events described in section 3, and the data-driven background distribution.

The top quark contribution is parameterised by a probability distribution function (pdf) which is the sum of a Novosibirsk function [43] and a Landau function [44]. These describe, respectively, the signal and the combinatorial background. As a first step,

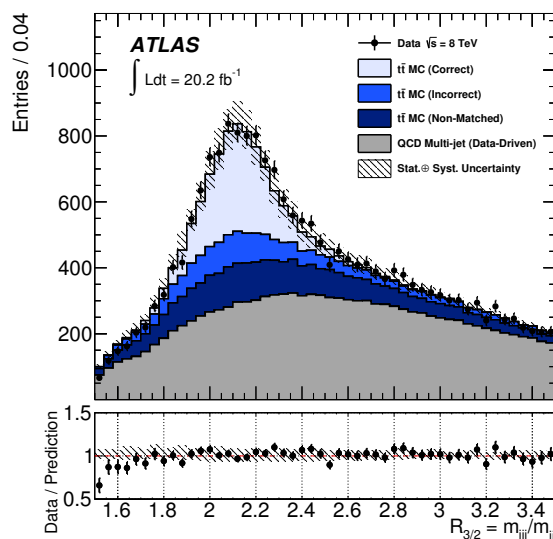


Figure 2. $R_{3/2}$ distribution as obtained after applying the analysis event selection shown together with the expected sum of $t\bar{t}$ simulation and multi-jet background. The distribution is shown before the χ^2 fit is applied. The ratio comparing data to prediction is shown below the figure. The hatched bands reflect the sum of the statistical and systematic errors added in quadrature. The $t\bar{t}$ simulation corresponds to $m_{\text{top}} = 172.5$ GeV.

the $R_{3/2}$ distributions from the five $t\bar{t}$ simulation samples with differing m_{top} are fitted separately to determine the six parameters for each template mass. The MC simulation shows that each of these parameters depends linearly on the input m_{top} . In the next step, the parameters are fitted to obtain the offsets and slopes of the linear m_{top} dependencies. These values are then used as inputs to a combined, simultaneous fit to all five $R_{3/2}$ distributions. In total 12 parameters are derived by the combined fit to determine the pdf. Figure 3 shows the $R_{3/2}$ distributions obtained using the $t\bar{t}$ MC samples based on the full simulation of the ATLAS detector and generated at three top-quark mass points: 167.5, 172.5, and 175 GeV. Results from the combined, simultaneous fit to all five $R_{3/2}$ distributions are superimposed. Shown are the functions describing the signal and combinatorial background, respectively, and their sum. The Novosibirsk mean and width parameters offer the strongest sensitivity to m_{top} . Template distributions obtained simultaneously for three separate input values of m_{top} (167.5, 172.5, and 177.5 GeV), highlighting the $R_{3/2}$ shape sensitivity to m_{top} , are shown in figure 4.

The multi-jet background template distribution obtained from the output of the data-driven method described in section 6 can be parameterised in a similar fashion. In this case the sum of a Gaussian function and a Landau function was found to be a suitable choice for the functional form. The background pdf requires five parameters.

As a final step in the parameterisation, in order to take properly into account the uncertainties and the correlations between the various signal and background shape parameters, a more generalised version of the χ^2 function is used. The final χ^2 fit, which uses

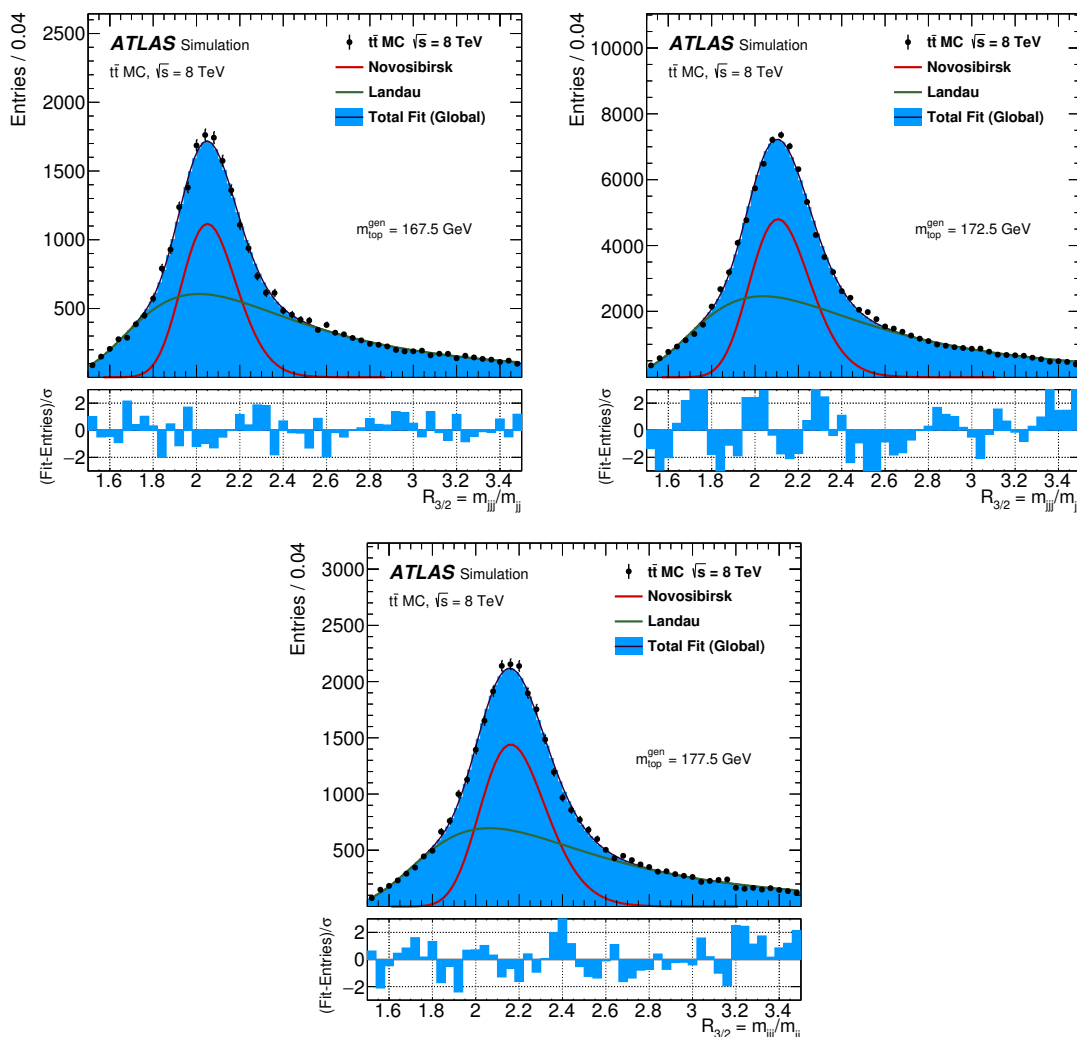


Figure 3. Templates for the $R_{3/2}$ distributions for $t\bar{t}$ MC samples generated at m_{top} values of 167.5, 172.5, and 177.5 GeV, respectively. Results from the combined, simultaneous fit to all five $R_{3/2}$ distributions are superimposed (black line with blue filled area). For each distribution it consists of a Novosibirsk function (red line) describing the signal part and a Landau function (green dashed-line) describing the combinatorial background part. Their parameters are assumed to depend linearly on m_{top} . The χ^2 per degree of freedom obtained for each of the three template distribution corresponds to 1.22, 3.98, and 1.96 respectively. The plot under each distribution shows the residuals obtained from calculating the difference between the combined fit and the simulated $R_{3/2}$ distribution normalised to the statistical uncertainty for each bin individually.

matrix algebra to include non-diagonal covariance matrices, has the form:

$$\chi^2 = \sum_{i=1}^{N_{\text{bin}}} \sum_{k=1}^{N_{\text{bin}}} (n_i - \mu_i) (n_k - \mu_k) [\mathbf{V}_{\text{data}} + \mathbf{V}_{\text{signal}}(m_{\text{top}}, F_{\text{bkgd}}) + \mathbf{V}_{\text{bkgd}}(F_{\text{bkgd}})]_{ik}^{-1}. \quad (7.1)$$

Here m_{top} and F_{bkgd} are the two parameters which are left to float. The shape of the fitted multi-jet background parameterisation is assumed to be independent of m_{top}

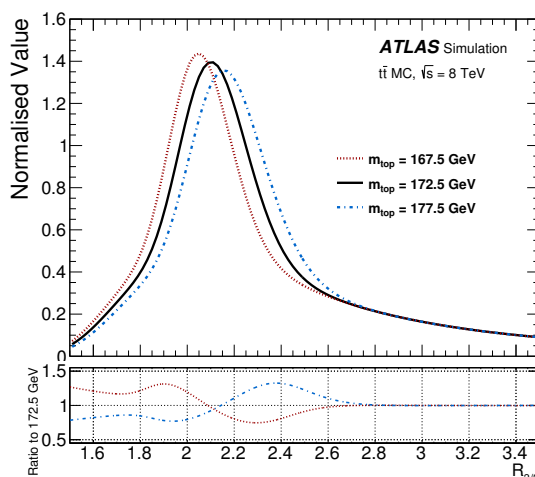


Figure 4. Template distributions shown simultaneously for three separate input values of m_{top} (167.5, 172.5, and 177.5 GeV), highlighting the sensitivity of the $R_{3/2}$ shape to m_{top} . The plot under the distribution shows the ratio of m_{top} at 167.5, and 177.5 GeV to m_{top} at 172.5 GeV.

while the normalisation, controlled by a background fraction parameter, F_{bkgd} , is obtained by fitting the data distribution. The F_{bkgd} is defined within the fit range of the $R_{3/2}$ distribution: $1.5 \leq R_{3/2} < 3.5$. The term n_i in eq. (7.1) corresponds to the number of entries in bin i in the $R_{3/2}$ data distribution, whereas μ_i corresponds to the estimated total number of signal and background entries. The term \mathbf{V}_{data} is the $N_{\text{bin}} \times N_{\text{bin}}$ diagonal data covariance matrix with $V_{ik} = \delta_{ik}n_i$, which accounts for the statistical uncertainty in each bin i . Similarly, $\mathbf{V}_{\text{signal}}$ and \mathbf{V}_{bkgd} are $N_{\text{bin}} \times N_{\text{bin}}$ non-diagonal covariance matrices which account for the signal and background shape parameterisation uncertainties and their correlations. In the $R_{3/2}$ distribution which has a total number of data entries N_d , and a given bin width w_{bin} , the number of estimated entries in bin i , μ_i , is given by:

$$\mu_i(m_{\text{top}}, F_{\text{bkgd}}) = w_{\text{bin}}N_d [(1 - F_{\text{bkgd}}) P_S(R_{3/2,i}|m_{\text{top}}) + F_{\text{bkgd}}P_B(R_{3/2,i})] \quad (7.2)$$

where P_S and P_B are the probability density functions for the signal and background, respectively.

8 Method validation and template closure

To validate the method employed to extract m_{top} from the $R_{3/2}$ data distribution and to check for any potential bias, a series of pseudo experiments are performed. For each of the five simulated m_{top} samples a total of 2500 pseudo experiments generating a distribution of the $R_{3/2}$ variable are produced.² Two scenarios are investigated: in the first one, events are drawn randomly from template $R_{3/2}$ distributions; in the second scenario, events are drawn directly from the signal and background shapes. In each scenario the nominal values

²This value of 2500 is also used when performing pseudo experiments to estimate the systematic uncertainties.

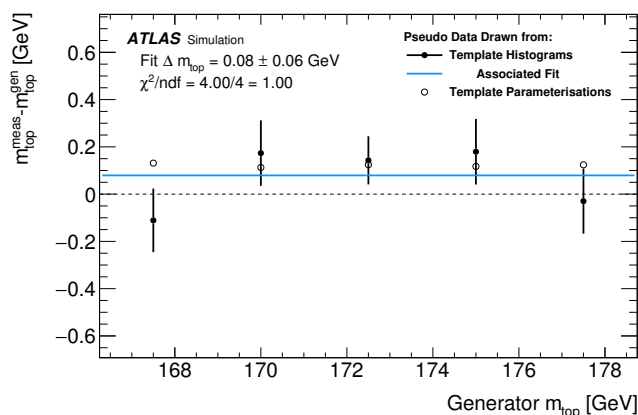


Figure 5. The difference mean, $(m_{\text{top}}^{\text{meas}} - m_{\text{top}}^{\text{gen}})$, based on the results of a fit to a single Gaussian function. The black markers correspond to cases where the pseudo events were drawn from the $R_{3/2}$ histograms, and the open marker points where pseudo events were drawn from the parameterisations. The solid blue line corresponds to a polynomial fit to the five black markers and their corrected uncertainties.

of all signal and background shape parameters are used, and only two parameter values, m_{top} and F_{bgd} , are returned from the minimisation procedure. For all five top-quark mass MC samples, the same multi-jet background distribution is used for drawing pseudo events.

The value of m_{top} obtained from each pseudo experiment ($m_{\text{top}}^{\text{meas}}$) is used to fill a distribution of the difference between these values and the values $m_{\text{top}}^{\text{gen}}$ used for event generation. This distribution is then fitted with a Gaussian function, giving estimators for the Gaussian mean and width parameters, each with their respective uncertainties. The uncertainty in the fitted mean is corrected for the oversampling that is induced by drawing from template distributions produced using a finite number of MC events [45]. The fitted mean $\langle(m_{\text{top}}^{\text{meas}} - m_{\text{top}}^{\text{gen}})\rangle$, referred to as the “difference mean”, is shown in figure 5. Fitting the difference mean for the five top-quark mass samples with a linear function gives an $m_{\text{top}}^{\text{gen}}$ -independent bias of 0.08 ± 0.06 GeV. The treatment of this small bias is further discussed in section 9.2.

Pull (z-score) distributions are constructed in an analogous way, where the pull in each pseudo experiment is defined as:

$$\text{Pull} = (m_{\text{top}}^{\text{meas}} - m_{\text{top}}^{\text{gen}}) / \delta m_{\text{top}}, \tag{8.1}$$

where δm_{top} is the statistical uncertainty of the m_{top} parameter obtained from the fit of the pseudo experiment. The correction that takes into account the correlation between two $R_{3/2}$ values in each event, described in section 7, is not applied here, as the values of $R_{3/2}$ drawn for pseudo experiments are uncorrelated. The pull distribution for an unbiased measurement has a mean of zero and a standard deviation of unity. A fitted pull mean value of 0.19 ± 0.13 and a fitted pull width of 0.98 ± 0.01 are obtained, which shows that the uncertainty determination is unbiased.

9 Systematic uncertainties

This section outlines the various sources of systematic uncertainty in m_{top} which are summarised in table 3. All sources are treated as uncorrelated. Individual contributions are symmetrised and the total uncertainty is taken as the sum in quadrature of all contributions.

The majority of the systematic uncertainties are assessed by varying the $t\bar{t}$ MC sample to reflect the uncertainty from each of these sources. Pseudo experiments are constructed from the varied sample, which are then passed through the analysis chain; the change in the result relative to that obtained from the nominal MC sample is evaluated. Exceptions to this are described in the following subsections. To facilitate a combination with other results, each systematic uncertainty is assigned a statistical uncertainty, taking into account the statistical correlation of the considered samples. Following ref. [46], the systematic uncertainties listed in table 3 are calculated independently of the statistical uncertainties of the values.

In what follows, each source of systematic uncertainty is briefly described. These are broken down into three categories. The first category, theory and modelling uncertainties, is associated with the simulation of the signal events. The second set of uncertainties is related to the analysis method. These involve uncertainties due to the way that the analysis was performed, including the choice of a template method, the background modelling, and the final m_{top} extraction procedure. Finally a third category, calibration- and detector-related uncertainties involves uncertainties coming from the standard calibrations of physics objects.

9.1 Theory and modelling uncertainties

Monte Carlo generator. In order to assess the impact on the m_{top} measurement due to the choice of MC generator, the results of pseudo experiments using two different AFII simulated samples are compared: one sample produced using POWHEG-BOX as the MC generator and a second sample using MC@NLO [47]. Both samples use HERWIG 6.520.2 [48] with the AUET2 tune to model the parton shower, hadronisation and underlying event, in contrast with the nominal signal MC where PYTHIA 6.427 is used. The absolute difference of 0.18 GeV between the resulting average m_{top} parameter returned from the fits is accounted for as the uncertainty.

Hadronisation modelling. To quantify the expected change in the measured m_{top} value due to a different choice of hadronisation model, pseudo experiments are performed for two independent MC samples both employing POWHEG-BOX AFII simulation to generate the all-hadronic $t\bar{t}$ events but differing in their choice of hadronisation model. In the first case, PYTHIA 6.427 [28] is used to model the parton shower, hadronisation and underlying event with the PERUGIA 2012 tunes [29], while in the second case, HERWIG 6.520.2 with the AUET2 tune [48] is used. The absolute difference of 0.64 GeV between the average m_{top} values obtained in the two cases is accounted for as the systematic uncertainty.

<i>Source of uncertainty</i>	Δm_{top} [GeV]
Monte Carlo generator	0.18 ± 0.21
Hadronisation modelling	0.64 ± 0.15
Parton distribution functions	0.04 ± 0.00
Initial/final-state radiation	0.10 ± 0.28
Underlying event	0.13 ± 0.16
Colour reconnection	0.12 ± 0.16
Bias in template method	0.06
Signal and bkgd parameterisation	0.09
Non all-hadronic $t\bar{t}$ contribution	0.06
ABCD method <i>vs.</i> ABCDEF method	0.16
Trigger efficiency	0.08 ± 0.01
Lepton/ $E_{\text{T}}^{\text{miss}}$ calibration	0.02 ± 0.01
Overall flavour-tagging	0.10 ± 0.00
Jet energy scale (JES)	0.60 ± 0.05
b-jet energy scale (bJES)	0.34 ± 0.02
Jet energy resolution	0.10 ± 0.04
Jet vertex fraction	0.03 ± 0.01
Total systematic uncertainty	1.01
Total statistical uncertainty	0.55
Total uncertainty	1.15

Table 3. Summary of all sources of statistical and systematic uncertainties in the measured values of the top-quark mass. Totals are evaluated by means of a sum in quadrature and assuming that all contributions are uncorrelated. The uncertainties are subdivided into three categories: theory and modelling uncertainties, method-related uncertainties, and calibration- or detector-related uncertainties, as described in the text. Adjacent to each of the quoted systematic variations in m_{top} is its associated statistical uncertainty. The ABCDEF method is further described in section 9.2 and in ref. [17]. The quoted statistical uncertainty is corrected for the correlation between the two $R_{3/2}$ measurements of each event.

Parton distribution functions A variety of PDF sets are investigated in order to assess the impact of the choice of CTEQ10 [26, 27], the default PDF set used in the nominal measurement. There are a total of 53 distinct sets for the CTEQ PDFs. In addition there are 101 distinct NNPDF23 [49] PDF sets and 41 distinct MSTW2008 [50, 51] PDF sets to consider, giving a total of 195 distinct sets to compare. Simulated POWHEG-BOX+HERWIG [23–25, 48] events are used for the comparison. The individual PDF uncertainty contributions are evaluated according to set-dependent procedures as described in ref. [52] for CT10 [26, 27], for MSTW [49], and for NNPDF [50, 51]. To determine the final systematic uncertainty, the quantities $m_{\text{top}} \pm \sigma_{m_{\text{top}}}$ are calculated for each of the three sets, where m_{top} is the measured value from the central reference sample of the corresponding PDF set, and $\sigma_{m_{\text{top}}}$ is the associated set-dependent uncertainty. Half of the difference between the largest and the smallest of these values is quoted as the symmetrised final uncertainty, and is 0.04 GeV.

Initial-state and final-state radiation. Varying the amount of initial- and final-state radiation (ISR and FSR) can have an impact on the number of reconstructed jets, which in turn can affect the overall measurement of the top-quark mass. In order to quantify the sensitivity of the measurement to ISR/FSR, two alternative POWHEG-BOX plus PYTHIA 6.427 [28] AFII samples are used. The first sample has the h_{damp} parameter [30] set to $2m_{\text{top}}$, the factorisation and renormalisation scale³ decreased by a factor of 0.5 and uses the PERUGIA 2012 RADHi tune [29], giving more parton shower radiation. The second sample has the PERUGIA 2012 RADLO tune, $h_{\text{damp}} = m_{\text{top}}$ and the factorisation and renormalisation scale increased by a factor of 2, giving less parton shower radiation. Half of the absolute difference between the measured m_{top} values from the pseudo experiments is quoted as the corresponding systematic uncertainty and is 0.10 GeV.

Underlying event. Additional semi-hard multiple parton interactions (MPI) present in the hard-scattering can change the kinematics of the underlying event. The number of such additional semi-hard MPI is a PERUGIA 2012 tunable parameter [29] in the PYTHIA 6.427 generator [28]. Simulated $t\bar{t}$ AFII events were produced with an increased number of semi-hard MPI (PERUGIA 2012 MPIHi) in order to assess the potential impact on the final measurement. The absolute difference between the results of these pseudo experiments and the one using the nominal simulated AFII sample is quoted as the systematic uncertainty and is 0.13 GeV.

Colour reconnection. When simulating AFII signal events using PYTHIA 6.427 [28] for the parton shower and hadronisation modelling, there is a tunable parameter associated with the colour reconnection strength due to the colour flow along parton lines in the strong-interaction hard-scattering process. An alternative AFII $t\bar{t}$ sample uses the PYTHIA PERUGIA 2012 LOCR tune [29], which corresponds to reduced colour reconnection strength. The absolute difference of 0.12 GeV between the results of these pseudo experiments and the average m_{top} value obtained using the nominal PYTHIA 6.427 $t\bar{t}$ events is quoted as the systematic uncertainty.

9.2 Method-dependent uncertainties

Bias in template method. Based on the results of the closure tests, a small bias is observed in the extracted top-quark mass. By drawing pseudo events from the parameterisations an offset of about 80 MeV in the mass difference ($m_{\text{top}}^{\text{meas}} - m_{\text{top}}^{\text{gen}}$) is present (see figure 5). The offset does not exhibit a dependence on the generator's m_{top} value. For this reason the parameter value returned from a fit to the average bias from pseudo experiments across $m_{\text{top}}^{\text{gen}}$ is subtracted from the final m_{top} value as measured in data. The final value of m_{top} quoted in this analysis includes this subtraction. The uncertainty in this fitted offset is then quoted as the systematic uncertainty of 0.06 GeV associated with the template method's non-closure.

³The default POWHEG-BOX factorisation and renormalisation scales are set to $\sqrt{m_{\text{top}}^2 + p_{\text{T}}^2}$.

Signal and background parameterisation. To extract m_{top} as described in section 7, the uncertainties in the shape parameters of the $R_{3/2}$ observable for the signal contributions are included in the $N_{\text{bin}} \times N_{\text{bin}}$ covariance matrices which enter into the χ^2 minimisation used to extract m_{top} (see eq. (7.1)). Omitting these contributions would yield a simplified definition of the χ^2 variable:

$$\chi^2 = \sum_{\text{bin } i}^{N_{\text{bin}}} \sum_{\text{bin } k}^{N_{\text{bin}}} (n_i - \mu_i) (n_k - \mu_k) [\mathbf{V}_{\text{data}}]_{ik}^{-1} = \sum_{\text{bin } i}^{N_{\text{bin}}} \frac{(n_i - \mu_i)^2}{n_i} \quad (9.1)$$

which can be recognised as the standard definition of the χ^2 variable for a least-squares fit assuming only a diagonal covariance matrix. The fit to the data distribution is repeated using this simplified definition of the χ^2 variable. This results in a slightly modified returned value of the m_{top} parameter and a smaller statistical uncertainty. The difference in quadrature of 0.09 GeV between the final statistical uncertainty returned from the original minimisation and this modified value is quoted as the uncertainty in the signal and background parameterisation.

Inclusion of non-all-hadronic $t\bar{t}$ background. A number of event selection requirements, such as the lepton veto and the requirement that $E_{\text{T}}^{\text{miss}} < 60$ GeV, result in a large suppression of background contributions arising from non-all-hadronic $t\bar{t}$ events. The estimated fractional contribution from such events in the final signal region is below 3%, and is not considered in the nominal case. Pseudo experiments are performed by drawing events from the nominal signal distribution but from a modified background, now consisting of QCD events and $t\bar{t}$ events with at least one leptonic W boson decay. The absolute difference of 0.06 GeV between the average m_{top} value obtained in this way and that from the nominal case is quoted as a systematic uncertainty.

Variation in the number of control regions. A variation of the background estimation procedure is considered in which six distinct regions, rather than four, are defined to estimate the multi-jet background. This is done by allowing three different values of $N_{b_{\text{tag}}}$: 0, 1, or ≥ 2 . Events can then be separated into the six differing regions as in the nominal analysis. As in the nominal case the number of b -tagged jets in an event considers only the leading six jets, ordered by p_{T} . The values of the second ABCD variable, $\langle \Delta\phi(b, W) \rangle$, are unchanged from the nominal case. One reason for considering this alternative is that the inclusion of a larger number of control regions could potentially provide sensitivity to different physics processes. Additionally, the systematic uncertainty contribution arising from uncertainties in the b -tagging scale factors could differ between these methods.

With a total of six regions shown in table 4 the background estimation technique remains similar to that using four regions.

The final SR is labelled F. The new region D, together with region B, is now used to predict the shape of the multi-jet background in SR F, whereas CR A, C, and E set the multi-jet background normalisation [17]. Pseudo experiments are performed by drawing background events from the modified multi-jet distribution in the final signal region. The absolute difference of 0.16 GeV between this and the nominal case is quoted as the systematic uncertainty.

Region	A	B	C	D	E	F
$N_{b_{\text{tag}}}$	0	0	1	1	≥ 2	≥ 2
$\langle \Delta\phi(b, W) \rangle$	≥ 2	< 2	≥ 2	< 2	≥ 2	< 2

Table 4. Definitions for each of the six regions ABCDEF used to estimate the multi-jet background.

9.3 Calibration- and detector-related uncertainties

Trigger efficiency. The trigger efficiency obtained using simulated signal events [23–25, 28, 29] is compared to an equivalent distribution obtained using data, which results in a small observed discrepancy. For the 5th jet $p_T > 68$ GeV the efficiencies for both simulation and data agree and are larger than 99%. In the 5th jet p_T region between 60 GeV and 68 GeV the signal simulation (data) efficiency is larger than 97% (90%) and rising with p_T . The data here are expected to consist primarily of multi-jet events. It is expected that some true kinematic differences give rise to the difference observed between the data and MC trigger efficiencies. In order to obtain a conservative uncertainty, it is assumed that the difference represents a mis-modelling of the data by the trigger simulation. The simulated events are assigned a p_T -dependent trigger efficiency correction such that the corrected MC and data trigger efficiencies agree. Pseudo experiments are performed by drawing signal events from the modified $R_{3/2}$ distribution with the trigger SFs applied, and the 0.08 GeV absolute difference from the nominal case is quoted as a conservative uncertainty on m_{top} due to the trigger efficiency.

Pile-up reweighting scale. The distribution of the average number of interactions per bunch crossing, denoted by $\langle \mu \rangle$, is known to differ between data and simulation. Simulated events are reweighted so that $\langle \mu \rangle$ matches the value observed in data. In order to assess the impact on the final result, pseudo experiments are performed in which the reweighting scale is shifted up and down according to its uncertainty, and the fit procedure is repeated. A negligible maximum change of 0.01 GeV in m_{top} is found as the symmetrised up/down uncertainty.

Lepton and E_T^{miss} soft-term calibrations. Uncertainties in the calibration scales and in the resolutions of the lepton (e/μ) four-vector objects [33, 53, 54] can potentially lead to small differences in the event selection or the jet-quark assignment in the top reconstruction algorithm. Similarly, small uncertainties in m_{top} can be expected due to the uncertainties in the scale and resolution of the E_T^{miss} soft term [39, 40]. The E_T^{miss} soft term is varied according to these uncertainties and pseudo experiments are performed with the modified MC events. In the case of the muon-related uncertainties, Gaussian smearing is performed to assess the impact on the final result. The maximum absolute deviation from the reference m_{top} value is taken as the uncertainty in each case, and these are added in quadrature to obtain a single value of 0.02 GeV for all lepton- and E_T^{miss} -related scale and resolution uncertainties.

Flavour-tagging efficiencies. In the validation of the flavour-tagging algorithms, the differences between tagging efficiencies and mis-tag rates evaluated in data and simulation are removed by applying scale factor (SF) weights to the simulated events. The uncertainties in the flavour-tagging SFs are calculated separately for the b -tagging SFs, the c/τ -tagging SFs, and the overall mis-tag SFs [42]. The uncertainties in the flavour-tagging SFs are split into various components. The full covariance matrix between the various bins of jet transverse momentum is built and decomposed into eigenvectors. Each eigenvector corresponds to an independent source of uncertainty, each with an upward and a downward fluctuation, and the resulting total systematic uncertainty is 0.10 GeV.

Jet energy scale. The different contributions to the total JES uncertainty are estimated individually as described in ref. [36]. For each component the resulting differences from the up and down variations, corresponding to one-standard-deviation relative to the nominal JES, are quoted separately. The total uncertainty for each contribution is taken as half of the absolute difference between the up and down variation. In case both the up and down variations result in a change in the parameter in the same direction, the largest absolute difference (either from the up or down variation) is taken as the symmetrised uncertainty. The total JES uncertainty is the sum in quadrature of all subcontributions, and is 0.60 GeV. This includes all but the b -jet energy scale contribution, which is quoted separately and discussed below.

b -jet energy scale. The reconstructed top quark four-momenta are sensitive to the energy scale of jets initiated by b -quarks, particularly as a result of choices in the fragmentation modelling. Based on the uncertainties associated with the b -jet energy scale [55], a similar up/down variation procedure is performed using pseudo experiments and the quoted systematic uncertainty of 0.34 GeV is half the absolute difference between the two variations.

Jet energy resolution. An eigenvector decomposition strategy similar to that followed for the JES and the flavour-tagging systematic uncertainties is used for the determination of jet energy resolution (JER) systematic uncertainties [56]. The final quoted JER systematic uncertainty is 0.10 GeV.

Jet reconstruction efficiency. A small difference between the jet reconstruction efficiencies measured in data and simulation was observed [37], and as this difference can affect the final measured m_{top} value, a set of pseudo experiments are performed in which jets from simulated events are removed at random. The frequency of this is chosen such that the modified jet reconstruction efficiency in simulation matches the value measured in data. The analysis is repeated with this change and no significant difference is observed.

10 Measurement of m_{top}

After applying the method described in section 7 the top-quark mass is measured to be:

$$m_{\text{top}} = 173.72 \pm 0.55 \text{ (stat.)} \pm 1.01 \text{ (syst.) GeV.} \quad (10.1)$$

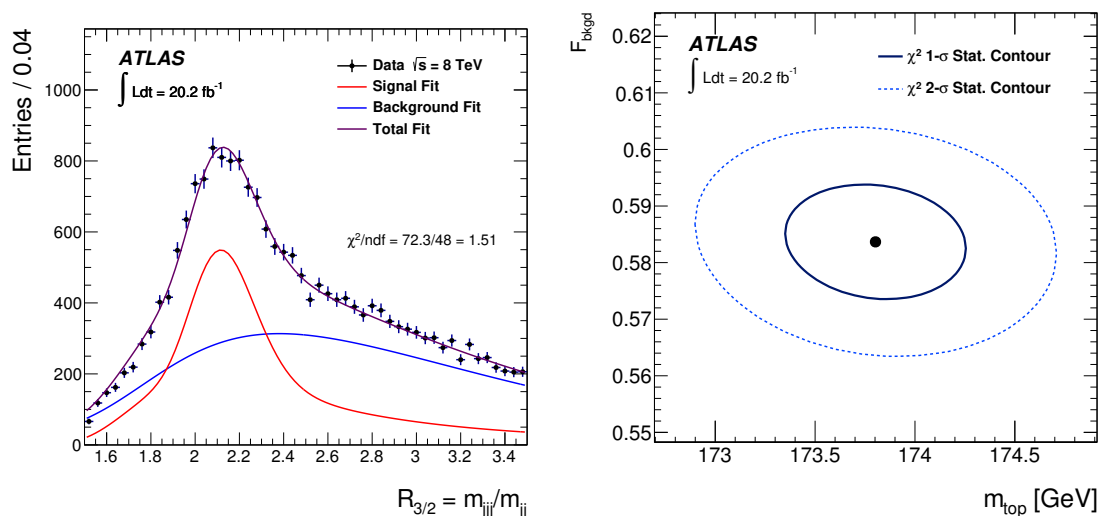


Figure 6. The left plot shows the $R_{3/2}$ distribution in data with the total fit (in magenta) and its decomposition into signal (in red) and the multi-jet background (in blue). The errors shown are statistical only. The right plot shows the ellipses corresponding to the 1- σ (solid line) and 2- σ (dashed line) statistical uncertainty. The central point in the figure indicates the values obtained for m_{top} on the x -axis, and the fitted background fraction, F_{bkgd} , obtained within the fit range of the $R_{3/2}$ distribution on the y -axis. The plots do not take into account the small bias correction described in section 9.2. The top-quark mass, after this correction, is 173.72 ± 0.55 (stat.) ± 1.01 (syst.) GeV.

The statistical error quoted in eq. (10.1) is corrected for the correlation between the two $R_{3/2}$ measurements of each event, as discussed in section 7. The systematic uncertainty quoted above is the sum in quadrature of all the systematic uncertainties described in section 9 and summarised in table 3. Figure 6 shows the $R_{3/2}$ distribution (left plot) with the corresponding total fit as well as its decomposition into signal and the multi-jet background. The right plot in this figure shows the ellipses corresponding to 1- σ (solid line) and 2- σ (dashed line) variations in statistical uncertainty. This measurement agrees with the previous all-hadronic m_{top} measurement performed by ATLAS in 7 TeV [17] data, with the m_{top} measurements performed in the single-lepton and dileptonic decay channels [11, 12, 14, 15] and with the results of combining the Tevatron and LHC measurements [13].

11 Conclusion

From the analysis of 20.2 fb^{-1} of data recorded with the ATLAS detector at the LHC at a pp centre-of-mass energy of 8 TeV, the top-quark mass has been measured in the all-hadronic decay channel of top-antitop quark pairs to be

$$m_{\text{top}} = 173.72 \pm 0.55 \text{ (stat.)} \pm 1.01 \text{ (syst.) GeV.} \tag{11.1}$$

This measurement is obtained from template fits to the $R_{3/2}$ observable, which is chosen due to its reduced dependence on the jet energy scale uncertainty. The dominant remaining

sources of systematic uncertainty, despite the usage of the $R_{3/2}$ observable, come from the jet energy scale, hadronisation modelling and the b -jet energy scale. This measurement agrees with the previous Tevatron and LHC m_{top} measurements, and with the results of Tevatron and LHC combinations. It is about 40% more precise than the previous m_{top} measurement performed by ATLAS in the all-hadronic channel at $\sqrt{s} = 7$ TeV.

Acknowledgments

We thank CERN for the very successful operation of the LHC, as well as the support staff from our institutions without whom ATLAS could not be operated efficiently.

We acknowledge the support of ANPCyT, Argentina; YerPhI, Armenia; ARC, Australia; BMWFW and FWF, Austria; ANAS, Azerbaijan; SSTC, Belarus; CNPq and FAPESP, Brazil; NSERC, NRC and CFI, Canada; CERN; CONICYT, Chile; CAS, MOST and NSFC, China; COLCIENCIAS, Colombia; MSMT CR, MPO CR and VSC CR, Czech Republic; DNRF and DNSRC, Denmark; IN2P3-CNRS, CEA-DSM/IRFU, France; SRNSF, Georgia; BMBF, HGF, and MPG, Germany; GSRT, Greece; RGC, Hong Kong SAR, China; ISF, I-CORE and Benoziyo Center, Israel; INFN, Italy; MEXT and JSPS, Japan; CNRST, Morocco; NWO, Netherlands; RCN, Norway; MNiSW and NCN, Poland; FCT, Portugal; MNE/IFA, Romania; MES of Russia and NRC KI, Russian Federation; JINR; MESTD, Serbia; MSSR, Slovakia; ARRS and MIZŠ, Slovenia; DST/NRF, South Africa; MINECO, Spain; SRC and Wallenberg Foundation, Sweden; SERI, SNSF and Cantons of Bern and Geneva, Switzerland; MOST, Taiwan; TAEK, Turkey; STFC, United Kingdom; DOE and NSF, United States of America. In addition, individual groups and members have received support from BCKDF, the Canada Council, CANARIE, CRC, Compute Canada, FQRNT, and the Ontario Innovation Trust, Canada; EPLANET, ERC, ERDF, FP7, Horizon 2020 and Marie Skłodowska-Curie Actions, European Union; Investissements d'avenir Labex and Idex, ANR, Région Auvergne and Fondation Partager le Savoir, France; DFG and AvH Foundation, Germany; Herakleitos, Thales and Aristeia programmes co-financed by EU-ESF and the Greek NSRF; BSF, GIF and Minerva, Israel; BRF, Norway; CERCA Programme Generalitat de Catalunya, Generalitat Valenciana, Spain; the Royal Society and Leverhulme Trust, United Kingdom.

The crucial computing support from all WLCG partners is acknowledged gratefully, in particular from CERN, the ATLAS Tier-1 facilities at TRIUMF (Canada), NDGF (Denmark, Norway, Sweden), CC-IN2P3 (France), KIT/GridKA (Germany), INFN-CNAF (Italy), NL-T1 (Netherlands), PIC (Spain), ASGC (Taiwan), RAL (U.K.) and BNL (U.S.A.), the Tier-2 facilities worldwide and large non-WLCG resource providers. Major contributors of computing resources are listed in ref. [57].

Open Access. This article is distributed under the terms of the Creative Commons Attribution License ([CC-BY 4.0](https://creativecommons.org/licenses/by/4.0/)), which permits any use, distribution and reproduction in any medium, provided the original author(s) and source are credited.

References

- [1] M. Kobayashi and T. Maskawa, *CP Violation in the Renormalizable Theory of Weak Interaction*, *Prog. Theor. Phys.* **49** (1973) 652 [INSPIRE].
- [2] CDF collaboration, F. Abe et al., *Observation of top quark production in $\bar{p}p$ collisions*, *Phys. Rev. Lett.* **74** (1995) 2626 [hep-ex/9503002] [INSPIRE].
- [3] D0 collaboration, S. Abachi et al., *Observation of the top quark*, *Phys. Rev. Lett.* **74** (1995) 2632 [hep-ex/9503003] [INSPIRE].
- [4] L. Evans and P. Bryant, *LHC Machine*, 2008 *JINST* **3** S08001 [INSPIRE].
- [5] T.D. Lee, *A theory of spontaneous t violation*, *Phys. Rev.* **D 8** (1973) 1226 [INSPIRE].
- [6] S. Weinberg, *Unitarity Constraints on CP Nonconservation in Higgs Exchange*, *Phys. Rev.* **D 42** (1990) 860 [INSPIRE].
- [7] W. Hollik, *Electroweak theory*, hep-ph/9602380 [INSPIRE].
- [8] M.E. Peskin, *On the Trail of the Higgs Boson*, *Annalen Phys.* **528** (2016) 20 [arXiv:1506.08185] [INSPIRE].
- [9] G. Degrandi et al., *Higgs mass and vacuum stability in the Standard Model at NNLO*, *JHEP* **08** (2012) 098 [arXiv:1205.6497] [INSPIRE].
- [10] GFITTER GROUP collaboration, M. Baak et al., *The global electroweak fit at NNLO and prospects for the LHC and ILC*, *Eur. Phys. J. C* **74** (2014) 3046 [arXiv:1407.3792] [INSPIRE].
- [11] CMS collaboration, *Measurement of the top quark mass using proton-proton data at $\sqrt{s} = 7$ and 8 TeV*, *Phys. Rev.* **D 93** (2016) 072004 [arXiv:1509.04044] [INSPIRE].
- [12] ATLAS collaboration, *Measurement of the top quark mass in the $t\bar{t} \rightarrow$ dilepton channel from $\sqrt{s} = 8$ TeV ATLAS data*, *Phys. Lett. B* **761** (2016) 350 [arXiv:1606.02179] [INSPIRE].
- [13] ATLAS, CDF, CMS, D0 collaborations, *First combination of Tevatron and LHC measurements of the top-quark mass*, arXiv:1403.4427 [INSPIRE].
- [14] D0 collaboration, V.M. Abazov et al., *Precision measurement of the top-quark mass in lepton+jets final states*, *Phys. Rev. Lett.* **113** (2014) 032002 [arXiv:1405.1756] [INSPIRE].
- [15] ATLAS collaboration, *Measurement of the top quark mass in the $t\bar{t} \rightarrow$ lepton+jets and $t\bar{t} \rightarrow$ dilepton channels using $\sqrt{s} = 7$ TeV ATLAS data*, *Eur. Phys. J. C* **75** (2015) 330 [arXiv:1503.05427] [INSPIRE].
- [16] PARTICLE DATA GROUP collaboration, K.A. Olive et al., *Review of Particle Physics*, *Chin. Phys. C* **38** (2014) 090001 [INSPIRE].
- [17] ATLAS collaboration, *Measurement of the top-quark mass in the fully hadronic decay channel from ATLAS data at $\sqrt{s} = 7$ TeV*, *Eur. Phys. J. C* **75** (2015) 158 [arXiv:1409.0832] [INSPIRE].
- [18] ATLAS collaboration, *The ATLAS Experiment at the CERN Large Hadron Collider*, 2008 *JINST* **3** S08003 [INSPIRE].
- [19] ATLAS collaboration, *The ATLAS Simulation Infrastructure*, *Eur. Phys. J. C* **70** (2010) 823 [arXiv:1005.4568] [INSPIRE].
- [20] GEANT4 collaboration, S. Agostinelli et al., *GEANT4: A simulation toolkit*, *Nucl. Instrum. Meth. A* **506** (2003) 250 [INSPIRE].

- [21] ATLAS collaboration, *The simulation principle and performance of the ATLAS fast calorimeter simulation FastCaloSim*, [ATL-PHYS-PUB-2010-013](#) (2010).
- [22] T. Sjöstrand, S. Mrenna and P.Z. Skands, *A Brief Introduction to PYTHIA 8.1*, *Comput. Phys. Commun.* **178** (2008) 852 [[arXiv:0710.3820](#)] [[INSPIRE](#)].
- [23] P. Nason, *A new method for combining NLO QCD with shower Monte Carlo algorithms*, *JHEP* **11** (2004) 040 [[hep-ph/0409146](#)] [[INSPIRE](#)].
- [24] S. Frixione, P. Nason and C. Oleari, *Matching NLO QCD computations with Parton Shower simulations: the POWHEG method*, *JHEP* **11** (2007) 070 [[arXiv:0709.2092](#)] [[INSPIRE](#)].
- [25] S. Alioli, P. Nason, C. Oleari and E. Re, *A general framework for implementing NLO calculations in shower Monte Carlo programs: the POWHEG BOX*, *JHEP* **06** (2010) 043 [[arXiv:1002.2581](#)] [[INSPIRE](#)].
- [26] H.-L. Lai et al., *New parton distributions for collider physics*, *Phys. Rev. D* **82** (2010) 074024 [[arXiv:1007.2241](#)] [[INSPIRE](#)].
- [27] J. Gao et al., *CT10 next-to-next-to-leading order global analysis of QCD*, *Phys. Rev. D* **89** (2014) 033009 [[arXiv:1302.6246](#)] [[INSPIRE](#)].
- [28] T. Sjöstrand, S. Mrenna and P.Z. Skands, *PYTHIA 6.4 Physics and Manual*, *JHEP* **05** (2006) 026 [[hep-ph/0603175](#)] [[INSPIRE](#)].
- [29] P.Z. Skands, *Tuning Monte Carlo Generators: The Perugia Tunes*, *Phys. Rev. D* **82** (2010) 074018 [[arXiv:1005.3457](#)] [[INSPIRE](#)].
- [30] ATLAS collaboration, *Comparison of Monte Carlo generator predictions for gap fraction and jet multiplicity observables in top-antitop events*, [ATL-PHYS-PUB-2014-005](#) (2014).
- [31] M. Czakon and A. Mitov, *Top++: A Program for the Calculation of the Top-Pair Cross-Section at Hadron Colliders*, *Comput. Phys. Commun.* **185** (2014) 2930 [[arXiv:1112.5675](#)] [[INSPIRE](#)].
- [32] ATLAS collaboration, *Electron performance measurements with the ATLAS detector using the 2010 LHC proton-proton collision data*, *Eur. Phys. J. C* **72** (2012) 1909 [[arXiv:1110.3174](#)] [[INSPIRE](#)].
- [33] ATLAS collaboration, *Measurement of the muon reconstruction performance of the ATLAS detector using 2011 and 2012 LHC proton-proton collision data*, *Eur. Phys. J. C* **74** (2014) 3130 [[arXiv:1407.3935](#)] [[INSPIRE](#)].
- [34] M. Cacciari, G.P. Salam and G. Soyez, *The anti- k_T jet clustering algorithm*, *JHEP* **04** (2008) 063 [[arXiv:0802.1189](#)] [[INSPIRE](#)].
- [35] ATLAS collaboration, *Topological cell clustering in the ATLAS calorimeters and its performance in LHC Run 1*, *Eur. Phys. J. C* **77** (2017) 490 [[arXiv:1603.02934](#)] [[INSPIRE](#)].
- [36] ATLAS collaboration, *Jet energy measurement and its systematic uncertainty in proton-proton collisions at $\sqrt{s} = 7$ TeV with the ATLAS detector*, *Eur. Phys. J. C* **75** (2015) 17 [[arXiv:1406.0076](#)] [[INSPIRE](#)].
- [37] ATLAS collaboration, *Jet energy measurement with the ATLAS detector in proton-proton collisions at $\sqrt{s} = 7$ TeV*, *Eur. Phys. J. C* **73** (2013) 2304 [[arXiv:1112.6426](#)] [[INSPIRE](#)].
- [38] ATLAS collaboration, *Performance of pile-up mitigation techniques for jets in pp collisions at $\sqrt{s} = 8$ TeV using the ATLAS detector*, *Eur. Phys. J. C* **76** (2016) 581 [[arXiv:1510.03823](#)] [[INSPIRE](#)].
- [39] ATLAS collaboration, *Performance of algorithms that reconstruct missing transverse momentum in $\sqrt{s} = 8$ TeV proton-proton collisions in the ATLAS detector*, *Eur. Phys. J. C* **77** (2017) 241 [[arXiv:1609.09324](#)] [[INSPIRE](#)].

- [40] ATLAS collaboration, *Pile-up Suppression in Missing Transverse Momentum Reconstruction in the ATLAS Experiment in Proton-Proton Collisions at $\sqrt{s} = 8$ TeV*, [ATLAS-CONF-2014-019](#) (2014).
- [41] ATLAS collaboration, *Commissioning of the ATLAS high-performance b-tagging algorithms in the 7 TeV collision data*, [ATLAS-CONF-2011-102](#) (2011).
- [42] ATLAS collaboration, *Calibration of the performance of b-tagging for c and light-flavour jets in the 2012 ATLAS data*, [ATLAS-CONF-2014-046](#) (2014).
- [43] BELLE collaboration, H. Ikeda et al., *A detailed test of the CsI(Tl) calorimeter for BELLE with photon beams of energy between 20-MeV and 5.4-GeV*, *Nucl. Instrum. Meth. A* **441** (2000) 401 [[INSPIRE](#)].
- [44] K.S. Kolbig and B. Schorr, *A Program Package for the Landau Distribution*, *Comput. Phys. Commun.* **31** (1984) 97 [*Erratum ibid.* **178** (2008) 972] [[INSPIRE](#)].
- [45] R.J. Barlow, *Application of the Bootstrap resampling technique to Particle Physics experiments*, MAN-HEP-99-4 (2000) [<http://www.hep.man.ac.uk/preprints/1999.html>].
- [46] R. Barlow, *Systematic errors: Facts and fictions*, [hep-ex/0207026](#) [[INSPIRE](#)].
- [47] S. Frixione and B.R. Webber, *Matching NLO QCD computations and parton shower simulations*, *JHEP* **06** (2002) 029 [[hep-ph/0204244](#)] [[INSPIRE](#)].
- [48] G. Corcella et al., *HERWIG 6: An Event generator for hadron emission reactions with interfering gluons (including supersymmetric processes)*, *JHEP* **01** (2001) 010 [[hep-ph/0011363](#)] [[INSPIRE](#)].
- [49] R.D. Ball et al., *Parton distributions with LHC data*, *Nucl. Phys. B* **867** (2013) 244 [[arXiv:1207.1303](#)] [[INSPIRE](#)].
- [50] A.D. Martin, W.J. Stirling, R.S. Thorne and G. Watt, *Parton distributions for the LHC*, *Eur. Phys. J. C* **63** (2009) 189 [[arXiv:0901.0002](#)] [[INSPIRE](#)].
- [51] A.D. Martin, W.J. Stirling, R.S. Thorne and G. Watt, *Uncertainties on α_s in global PDF analyses and implications for predicted hadronic cross sections*, *Eur. Phys. J. C* **64** (2009) 653 [[arXiv:0905.3531](#)] [[INSPIRE](#)].
- [52] M. Botje et al., *The PDF4LHC Working Group Interim Recommendations*, [arXiv:1101.0538](#) [[INSPIRE](#)].
- [53] ATLAS collaboration, *Electron reconstruction and identification efficiency measurements with the ATLAS detector using the 2011 LHC proton-proton collision data*, *Eur. Phys. J. C* **74** (2014) 2941 [[arXiv:1404.2240](#)] [[INSPIRE](#)].
- [54] ATLAS collaboration, *Electron and photon energy calibration with the ATLAS detector using LHC Run 1 data*, *Eur. Phys. J. C* **74** (2014) 3071 [[arXiv:1407.5063](#)] [[INSPIRE](#)].
- [55] ATLAS collaboration, *Jet energy measurement and systematic uncertainties using tracks for jets and for b-quark jets produced in proton-proton collisions at $\sqrt{s} = 7$ TeV in the ATLAS detector*, [ATLAS-CONF-2013-002](#) (2013).
- [56] ATLAS collaboration, *Monte Carlo Calibration and Combination of In-situ Measurements of Jet Energy Scale, Jet Energy Resolution and Jet Mass in ATLAS*, [ATLAS-CONF-2015-037](#) (2015).
- [57] ATLAS collaboration, *ATLAS Computing Acknowledgements 2016–2017*, [ATL-GEN-PUB-2016-002](#) (2016).

The ATLAS collaboration

M. Aaboud^{137d}, G. Aad⁸⁸, B. Abbott¹¹⁵, J. Abdallah⁸, O. Abdinov¹², B. Abeloos¹¹⁹, R. Aben¹⁰⁹, O.S. AbouZeid¹³⁹, N.L. Abraham¹⁵¹, H. Abramowicz¹⁵⁵, H. Abreu¹⁵⁴, R. Abreu¹¹⁸, Y. Abulaiti^{148a,148b}, B.S. Acharya^{167a,167b,a}, S. Adachi¹⁵⁷, L. Adamczyk^{41a}, D.L. Adams²⁷, J. Adelman¹¹⁰, S. Adomeit¹⁰², T. Adye¹³³, A.A. Affolder⁷⁷, T. Agatonovic-Jovin¹⁴, J.A. Aguilar-Saavedra^{128a,128f}, S.P. Ahlen²⁴, F. Ahmadov^{68,b}, G. Aielli^{135a,135b}, H. Akerstedt^{148a,148b}, T.P.A. Åkesson⁸⁴, A.V. Akimov⁹⁸, G.L. Alberghi^{22a,22b}, J. Albert¹⁷², S. Albrand⁵⁸, M.J. Alconada Verzini⁷⁴, M. Aleksa³², I.N. Aleksandrov⁶⁸, C. Alexa^{28b}, G. Alexander¹⁵⁵, T. Alexopoulos¹⁰, M. Alhroob¹¹⁵, B. Ali¹³⁰, M. Aliev^{76a,76b}, G. Alimonti^{94a}, J. Alison³³, S.P. Alkire³⁸, B.M.M. Allbrooke¹⁵¹, B.W. Allen¹¹⁸, P.P. Allport¹⁹, A. Aloisio^{106a,106b}, A. Alonso³⁹, F. Alonso⁷⁴, C. Alpigiani¹⁴⁰, A.A. Alshehri⁵⁶, M. Alstаты⁸⁸, B. Alvarez Gonzalez³², D. Álvarez Piqueras¹⁷⁰, M.G. Alviggi^{106a,106b}, B.T. Amadio¹⁶, Y. Amaral Coutinho^{26a}, C. Amelung²⁵, D. Amidei⁹², S.P. Amor Dos Santos^{128a,128c}, A. Amorim^{128a,128b}, S. Amoroso³², G. Amundsen²⁵, C. Anastopoulos¹⁴¹, L.S. Ancu⁵², N. Andari¹⁹, T. Andeen¹¹, C.F. Anders^{60b}, G. Anders³², J.K. Anders⁷⁷, K.J. Anderson³³, A. Andreazza^{94a,94b}, V. Andrei^{60a}, S. Angelidakis⁹, I. Angelozzi¹⁰⁹, A. Angerami³⁸, F. Anghinolfi³², A.V. Anisenkov^{111,c}, N. Anjos¹³, A. Annovi^{126a,126b}, C. Antel^{60a}, M. Antonelli⁵⁰, A. Antonov^{100,*}, D.J. Antrim¹⁶⁶, F. Anulli^{134a}, M. Aoki⁶⁹, L. Aperio Bella¹⁹, G. Arabidze⁹³, Y. Arai⁶⁹, J.P. Araque^{128a}, A.T.H. Arce⁴⁸, F.A. Arduh⁷⁴, J-F. Arguin⁹⁷, S. Argyropoulos⁶⁶, M. Arik^{20a}, A.J. Armbruster¹⁴⁵, L.J. Armitage⁷⁹, O. Arnaez³², H. Arnold⁵¹, M. Arratia³⁰, O. Arslan²³, A. Artamonov⁹⁹, G. Artoni¹²², S. Artz⁸⁶, S. Asai¹⁵⁷, N. Asbah⁴⁵, A. Ashkenazi¹⁵⁵, B. Åsman^{148a,148b}, L. Asquith¹⁵¹, K. Assamagan²⁷, R. Astalos^{146a}, M. Atkinson¹⁶⁹, N.B. Atlay¹⁴³, K. Augsten¹³⁰, G. Avolio³², B. Axen¹⁶, M.K. Ayoub¹¹⁹, G. Azuelos^{97,d}, M.A. Baak³², A.E. Baas^{60a}, M.J. Baca¹⁹, H. Bachacou¹³⁸, K. Bachas^{76a,76b}, M. Backes¹²², M. Backhaus³², P. Bagiachi^{134a,134b}, P. Bagnaia^{134a,134b}, Y. Bai^{35a}, J.T. Baines¹³³, M. Bajic³⁹, O.K. Baker¹⁷⁹, E.M. Baldin^{111,c}, P. Balek¹⁷⁵, T. Balestri¹⁵⁰, F. Balli¹³⁸, W.K. Balunas¹²⁴, E. Banas⁴², Sw. Banerjee^{176,e}, A.A.E. Bannoura¹⁷⁸, L. Barak³², E.L. Barberio⁹¹, D. Barberis^{53a,53b}, M. Barbero⁸⁸, T. Barillari¹⁰³, M-S Barisits³², T. Barklow¹⁴⁵, N. Barlow³⁰, S.L. Barnes⁸⁷, B.M. Barnett¹³³, R.M. Barnett¹⁶, Z. Barnovska-Blenessy^{36a}, A. Baroncelli^{136a}, G. Barone²⁵, A.J. Barr¹²², L. Barranco Navarro¹⁷⁰, F. Barreiro⁸⁵, J. Barreiro Guimarães da Costa^{35a}, R. Bartoldus¹⁴⁵, A.E. Barton⁷⁵, P. Bartos^{146a}, A. Basalaeв¹²⁵, A. Bassalat^{119,f}, R.L. Bates⁵⁶, S.J. Batista¹⁶¹, J.R. Batley³⁰, M. Battaglia¹³⁹, M. Bauce^{134a,134b}, F. Bauer¹³⁸, H.S. Bawa^{145,g}, J.B. Beacham¹¹³, M.D. Beattie⁷⁵, T. Beau⁸³, P.H. Beauchemin¹⁶⁵, P. Bechtel²³, H.P. Beck^{18,h}, K. Becker¹²², M. Becker⁸⁶, M. Beckingham¹⁷³, C. Becot¹¹², A.J. Beddall^{20e}, A. Beddall^{20b}, V.A. Bednyakov⁶⁸, M. Bedognetti¹⁰⁹, C.P. Bee¹⁵⁰, L.J. Beamster¹⁰⁹, T.A. Beermann³², M. Begel²⁷, J.K. Behr⁴⁵, A.S. Bell⁸¹, G. Bella¹⁵⁵, L. Bellagamba^{22a}, A. Bellerive³¹, M. Bellomo⁸⁹, K. Belotskiy¹⁰⁰, O. Beltramello³², N.L. Belyaev¹⁰⁰, O. Benary^{155,*}, D. Bencheikroun^{137a}, M. Bender¹⁰², K. Bendtz^{148a,148b}, N. Benekos¹⁰, Y. Benhammou¹⁵⁵, E. Benhar Noccioli¹⁷⁹, J. Benitez⁶⁶, D.P. Benjamin⁴⁸, J.R. Bensinger²⁵, S. Bentvelsen¹⁰⁹, L. Beresford¹²², M. Beretta⁵⁰, D. Berge¹⁰⁹, E. Bergeas Kuutmann¹⁶⁸, N. Berger⁵, J. Beringer¹⁶, S. Berlendis⁵⁸, N.R. Bernard⁸⁹, C. Bernius¹¹², F.U. Bernlochner²³, T. Berry⁸⁰, P. Berta¹³¹, C. Bertella⁸⁶, G. Bertoli^{148a,148b}, F. Bertolucci^{126a,126b}, I.A. Bertram⁷⁵, C. Bertsche⁴⁵, D. Bertsche¹¹⁵, G.J. Besjes³⁹, O. Bessidskaia Bylund^{148a,148b}, M. Bessner⁴⁵, N. Besson¹³⁸, C. Betancourt⁵¹, A. Bethani⁵⁸, S. Bethke¹⁰³, A.J. Bevan⁷⁹, R.M. Bianchi¹²⁷, M. Bianco³², O. Biebel¹⁰², D. Biedermann¹⁷, R. Bielski⁸⁷, N.V. Biesuz^{126a,126b}, M. Biglietti^{136a}, J. Bilbao De Mendizabal⁵², T.R.V. Billoud⁹⁷, H. Bilokon⁵⁰, M. Bindi⁵⁷, A. Bingul^{20b}, C. Bini^{134a,134b}, S. Biondi^{22a,22b}, T. Bisanz⁵⁷,

D.M. Bjergaard⁴⁸, C.W. Black¹⁵², J.E. Black¹⁴⁵, K.M. Black²⁴, D. Blackburn¹⁴⁰, R.E. Blair⁶,
 T. Blazek^{146a}, I. Bloch⁴⁵, C. Blocker²⁵, A. Blue⁵⁶, W. Blum^{86,*}, U. Blumenschein⁵⁷,
 S. Blunier^{34a}, G.J. Bobbink¹⁰⁹, V.S. Bobrovnikov^{111,c}, S.S. Bocchetta⁸⁴, A. Bocci⁴⁸, C. Bock¹⁰²,
 M. Boehler⁵¹, D. Boerner¹⁷⁸, J.A. Bogaerts³², D. Bogavac¹⁴, A.G. Bogdanchikov¹¹¹,
 C. Bohm^{148a}, V. Boisvert⁸⁰, P. Bokan¹⁴, T. Bold^{41a}, A.S. Boldyrev¹⁰¹, M. Bomben⁸³, M. Bona⁷⁹,
 M. Boonekamp¹³⁸, A. Borisov¹³², G. Borissov⁷⁵, J. Bortfeldt³², D. Bortoletto¹²²,
 V. Bortolotto^{62a,62b,62c}, K. Bos¹⁰⁹, D. Boscherini^{22a}, M. Bosman¹³, J.D. Bossio Sola²⁹,
 J. Boudreau¹²⁷, J. Bouffard², E.V. Bouhova-Thacker⁷⁵, D. Boumediene³⁷, C. Bourdarios¹¹⁹,
 S.K. Boutle⁵⁶, A. Boveia³², J. Boyd³², I.R. Boyko⁶⁸, J. Bracinik¹⁹, A. Brandt⁸, G. Brandt⁵⁷,
 O. Brandt^{60a}, U. Bratzler¹⁵⁸, B. Brau⁸⁹, J.E. Brau¹¹⁸, W.D. Breaden Madden⁵⁶,
 K. Brendlinger¹²⁴, A.J. Brennan⁹¹, L. Brenner¹⁰⁹, R. Brenner¹⁶⁸, S. Bressler¹⁷⁵, T.M. Bristow⁴⁹,
 D. Britton⁵⁶, D. Britzger⁴⁵, F.M. Brochu³⁰, I. Brock²³, R. Brock⁹³, G. Brooijmans³⁸,
 T. Brooks⁸⁰, W.K. Brooks^{34b}, J. Brosamer¹⁶, E. Brost¹¹⁰, J.H. Broughton¹⁹,
 P.A. Bruckman de Renstrom⁴², D. Bruncko^{146b}, R. Bruneliere⁵¹, A. Bruni^{22a}, G. Bruni^{22a},
 L.S. Bruni¹⁰⁹, B.H. Brunt³⁰, M. Bruschi^{22a}, N. Brusino²³, P. Bryant³³, L. Bryngemark⁸⁴,
 T. Buanes¹⁵, Q. Buat¹⁴⁴, P. Buchholz¹⁴³, A.G. Buckley⁵⁶, I.A. Budagov⁶⁸, F. Buehrer⁵¹,
 M.K. Bugge¹²¹, O. Bulekov¹⁰⁰, D. Bullock⁸, H. Burckhart³², S. Burdin⁷⁷, C.D. Burgard⁵¹,
 B. Burghgrave¹¹⁰, K. Burka⁴², S. Burke¹³³, I. Burmeister⁴⁶, J.T.P. Burr¹²², E. Busato³⁷,
 D. B scher⁵¹, V. B scher⁸⁶, P. Bussey⁵⁶, J.M. Butler²⁴, C.M. Buttar⁵⁶, J.M. Butterworth⁸¹,
 P. Butti¹⁰⁹, W. Buttinger²⁷, A. Buzatu⁵⁶, A.R. Buzykaev^{111,c}, S. Cabrera Urb n¹⁷⁰,
 D. Caforio¹³⁰, V.M. Cairo^{40a,40b}, O. Cakir^{4a}, N. Calace⁵², P. Calafiura¹⁶, A. Calandri⁸⁸,
 G. Calderini⁸³, P. Calfayan⁶⁴, G. Callea^{40a,40b}, L.P. Caloba^{26a}, S. Calvente Lopez⁸⁵, D. Calvet³⁷,
 S. Calvet³⁷, T.P. Calvet⁸⁸, R. Camacho Toro³³, S. Camarda³², P. Camarri^{135a,135b},
 D. Cameron¹²¹, R. Caminal Armadans¹⁶⁹, C. Camincher⁵⁸, S. Campana³², M. Campanelli⁸¹,
 A. Camplani^{94a,94b}, A. Campoverde¹⁴³, V. Canale^{106a,106b}, A. Canepa^{163a}, M. Cano Bret^{36c},
 J. Cantero¹¹⁶, T. Cao⁴³, M.D.M. Capeans Garrido³², I. Caprini^{28b}, M. Caprini^{28b},
 M. Capua^{40a,40b}, R.M. Carbone³⁸, R. Cardarelli^{135a}, F. Cardillo⁵¹, I. Carli¹³¹, T. Carli³²,
 G. Carlino^{106a}, L. Carminati^{94a,94b}, R.M.D. Carney^{148a,148b}, S. Caron¹⁰⁸, E. Carquin^{34b},
 G.D. Carrillo-Montoya³², J.R. Carter³⁰, J. Carvalho^{128a,128c}, D. Casadei¹⁹, M.P. Casado^{13,i},
 M. Casolino¹³, D.W. Casper¹⁶⁶, E. Castaneda-Miranda^{147a}, R. Castelijm¹⁰⁹, A. Castelli¹⁰⁹,
 V. Castillo Gimenez¹⁷⁰, N.F. Castro^{128a,j}, A. Catinaccio³², J.R. Catmore¹²¹, A. Cattai³²,
 J. Caudron²³, V. Cavaliere¹⁶⁹, E. Cavallaro¹³, D. Cavalli^{94a}, M. Cavalli-Sforza¹³,
 V. Cavasinni^{126a,126b}, F. Ceradini^{136a,136b}, L. Cerda Alberich¹⁷⁰, A.S. Cerqueira^{26b}, A. Cerri¹⁵¹,
 L. Cerrito^{135a,135b}, F. Cerutti¹⁶, A. Cervelli¹⁸, S.A. Cetin^{20d}, A. Chafaq^{137a}, D. Chakraborty¹¹⁰,
 S.K. Chan⁵⁹, Y.L. Chan^{62a}, P. Chang¹⁶⁹, J.D. Chapman³⁰, D.G. Charlton¹⁹, A. Chatterjee⁵²,
 C.C. Chau¹⁶¹, C.A. Chavez Barajas¹⁵¹, S. Che¹¹³, S. Cheatham^{167a,167c}, A. Chegwidden⁹³,
 S. Chekanov⁶, S.V. Chekulaev^{163a}, G.A. Chelkov^{68,k}, M.A. Chelstowska⁹², C. Chen⁶⁷, H. Chen²⁷,
 K. Chen¹⁵⁰, S. Chen^{35b}, S. Chen¹⁵⁷, X. Chen^{35c}, Y. Chen⁷⁰, H.C. Cheng⁹², H.J. Cheng^{35a},
 Y. Cheng³³, A. Cheplakov⁶⁸, E. Cheremushkina¹³², R. Cherkaoui El Moursli^{137e},
 V. Chernyatin^{27,*}, E. Cheu⁷, L. Chevalier¹³⁸, V. Chiarella⁵⁰, G. Chiarelli^{126a,126b},
 G. Chiodini^{76a}, A.S. Chisholm³², A. Chitan^{28b}, M.V. Chizhov⁶⁸, K. Choi⁶⁴, A.R. Chomont³⁷,
 S. Chouridou⁹, B.K.B. Chow¹⁰², V. Christodoulou⁸¹, D. Chromek-Burckhart³², J. Chudoba¹²⁹,
 A.J. Chuinard⁹⁰, J.J. Chwastowski⁴², L. Chytka¹¹⁷, G. Ciapetti^{134a,134b}, A.K. Ciftci^{4a},
 D. Cinca⁴⁶, V. Cindro⁷⁸, I.A. Cioara²³, C. Ciocca^{22a,22b}, A. Ciocio¹⁶, F. Ciroto^{106a,106b},
 Z.H. Citron¹⁷⁵, M. Citterio^{94a}, M. Ciubancan^{28b}, A. Clark⁵², B.L. Clark⁵⁹, M.R. Clark³⁸,
 P.J. Clark⁴⁹, R.N. Clarke¹⁶, C. Clement^{148a,148b}, Y. Coadou⁸⁸, M. Cokal^{167a,167c}, A. Coccaro⁵²,
 J. Cochran⁶⁷, L. Colasurdo¹⁰⁸, B. Cole³⁸, A.P. Colijn¹⁰⁹, J. Collot⁵⁸, T. Colombo¹⁶⁶,
 G. Compostella¹⁰³, P. Conde Mui n^{128a,128b}, E. Coniavitis⁵¹, S.H. Connell^{147b}, I.A. Connelly⁸⁰,

V. Consorti⁵¹, S. Constantinescu^{28b}, G. Conti³², F. Conventi^{106a,l}, M. Cooke¹⁶, B.D. Cooper⁸¹, A.M. Cooper-Sarkar¹²², F. Cormier¹⁷¹, K.J.R. Cormier¹⁶¹, T. Cornelissen¹⁷⁸, M. Corradi^{134a,134b}, F. Corriveau^{90,m}, A. Cortes-Gonzalez³², G. Cortiana¹⁰³, G. Costa^{94a}, M.J. Costa¹⁷⁰, D. Costanzo¹⁴¹, G. Cottin³⁰, G. Cowan⁸⁰, B.E. Cox⁸⁷, K. Cranmer¹¹², S.J. Crawley⁵⁶, G. Cree³¹, S. Crépé-Renaudin⁵⁸, F. Crescioli⁸³, W.A. Cribbs^{148a,148b}, M. Crispin Ortuzar¹²², M. Cristinziani²³, V. Croft¹⁰⁸, G. Crosetti^{40a,40b}, A. Cueto⁸⁵, T. Cuhadar Donszelmann¹⁴¹, J. Cummings¹⁷⁹, M. Curatolo⁵⁰, J. Cúth⁸⁶, H. Czirr¹⁴³, P. Czodrowski³, G. D'amen^{22a,22b}, S. D'Auria⁵⁶, M. D'Onofrio⁷⁷, M.J. Da Cunha Sargedas De Sousa^{128a,128b}, C. Da Via⁸⁷, W. Dabrowski^{41a}, T. Dado^{146a}, T. Dai⁹², O. Dale¹⁵, F. Dallaire⁹⁷, C. Dallapiccola⁸⁹, M. Dam³⁹, J.R. Dandoy³³, N.P. Dang⁵¹, A.C. Daniells¹⁹, N.S. Dann⁸⁷, M. Danninger¹⁷¹, M. Dano Hoffmann¹³⁸, V. Dao⁵¹, G. Darbo^{53a}, S. Darmora⁸, J. Dassoulas³, A. Dattagupta¹¹⁸, W. Davey²³, C. David¹⁷², T. Davidek¹³¹, M. Davies¹⁵⁵, P. Davison⁸¹, E. Dawe⁹¹, I. Dawson¹⁴¹, K. De⁸, R. de Asmundis^{106a}, A. De Benedetti¹¹⁵, S. De Castro^{22a,22b}, S. De Cecco⁸³, N. De Groot¹⁰⁸, P. de Jong¹⁰⁹, H. De la Torre⁹³, F. De Lorenzi⁶⁷, A. De Maria⁵⁷, D. De Pedis^{134a}, A. De Salvo^{134a}, U. De Sanctis¹⁵¹, A. De Santo¹⁵¹, J.B. De Vivie De Regie¹¹⁹, W.J. Dearnaley⁷⁵, R. Debbe²⁷, C. Debenedetti¹³⁹, D.V. Dedovich⁶⁸, N. Dehghanian³, I. Deigaard¹⁰⁹, M. Del Gaudio^{40a,40b}, J. Del Peso⁸⁵, T. Del Prete^{126a,126b}, D. Delgove¹¹⁹, F. Deliot¹³⁸, C.M. Delitzsch⁵², A. Dell'Acqua³², L. Dell'Asta²⁴, M. Dell'Orso^{126a,126b}, M. Della Pietra^{106a,l}, D. della Volpe⁵², M. Delmastro⁵, P.A. Delsart⁵⁸, D.A. DeMarco¹⁶¹, S. Demers¹⁷⁹, M. Demichev⁶⁸, A. Demilly⁸³, S.P. Denisov¹³², D. Denysiuk¹³⁸, D. Derendarz⁴², J.E. Derkaoui^{137d}, F. Derue⁸³, P. Dervan⁷⁷, K. Desch²³, C. Deterre⁴⁵, K. Dette⁴⁶, P.O. Deviveiros³², A. Dewhurst¹³³, S. Dhaliwal²⁵, A. Di Ciaccio^{135a,135b}, L. Di Ciaccio⁵, W.K. Di Clemente¹²⁴, C. Di Donato^{106a,106b}, A. Di Girolamo³², B. Di Girolamo³², B. Di Micco^{136a,136b}, R. Di Nardo³², A. Di Simone⁵¹, R. Di Sipio¹⁶¹, D. Di Valentino³¹, C. Diaconu⁸⁸, M. Diamond¹⁶¹, F.A. Dias⁴⁹, M.A. Diaz^{34a}, E.B. Diehl⁹², J. Dietrich¹⁷, S. Díez Cornell⁴⁵, A. Dimitrievska¹⁴, J. Dingfelder²³, P. Dita^{28b}, S. Dita^{28b}, F. Dittus³², F. Djama⁸⁸, T. Djobava^{54b}, J.I. Djuvsland^{60a}, M.A.B. do Vale^{26c}, D. Dobos³², M. Dobre^{28b}, C. Doglioni⁸⁴, J. Dolejsi¹³¹, Z. Dolezal¹³¹, M. Donadelli^{26d}, S. Donati^{126a,126b}, P. Dondero^{123a,123b}, J. Donini³⁷, J. Dopke¹³³, A. Doria^{106a}, M.T. Dova⁷⁴, A.T. Doyle⁵⁶, E. Drechsler⁵⁷, M. Dris¹⁰, Y. Du^{36b}, J. Duarte-Camperderros¹⁵⁵, E. Duchovni¹⁷⁵, G. Duckeck¹⁰², O.A. Ducu^{97,n}, D. Duda¹⁰⁹, A. Dudarev³², A.Ch. Dudder⁸⁶, E.M. Duffield¹⁶, L. Duflot¹¹⁹, M. Dührssen³², M. Dumancic¹⁷⁵, A.K. Duncan⁵⁶, M. Dunford^{60a}, H. Duran Yildiz^{4a}, M. Düren⁵⁵, A. Durglishvili^{54b}, D. Duschinger⁴⁷, B. Dutta⁴⁵, M. Dyndal⁴⁵, C. Eckardt⁴⁵, K.M. Ecker¹⁰³, R.C. Edgar⁹², N.C. Edwards⁴⁹, T. Eifert³², G. Eigen¹⁵, K. Einsweiler¹⁶, T. Ekelof¹⁶⁸, M. El Kacimi^{137c}, V. Ellajosyula⁸⁸, M. Ellert¹⁶⁸, S. Elles⁵, F. Ellinghaus¹⁷⁸, A.A. Elliot¹⁷², N. Ellis³², J. Elmsheuser²⁷, M. Elsing³², D. Emeliyanov¹³³, Y. Enari¹⁵⁷, O.C. Endner⁸⁶, J.S. Ennis¹⁷³, J. Erdmann⁴⁶, A. Ereditato¹⁸, G. Ernis¹⁷⁸, J. Ernst², M. Ernst²⁷, S. Errede¹⁶⁹, E. Ertel⁸⁶, M. Escalier¹¹⁹, H. Esch⁴⁶, C. Escobar¹²⁷, B. Esposito⁵⁰, A.I. Etienvre¹³⁸, E. Etzion¹⁵⁵, H. Evans⁶⁴, A. Ezhilov¹²⁵, M. Ezzi^{137e}, F. Fabbri^{22a,22b}, L. Fabbri^{22a,22b}, G. Facini³³, R.M. Fakhruddinov¹³², S. Falciano^{134a}, R.J. Falla⁸¹, J. Faltova³², Y. Fang^{35a}, M. Fanti^{94a,94b}, A. Farbin⁸, A. Farilla^{136a}, C. Farina¹²⁷, E.M. Farina^{123a,123b}, T. Farooque¹³, S. Farrell¹⁶, S.M. Farrington¹⁷³, P. Farthouat³², F. Fassi^{137e}, P. Fassnacht³², D. Fassouliotis⁹, M. Faucci Giannelli⁸⁰, A. Favareto^{53a,53b}, W.J. Fawcett¹²², L. Fayard¹¹⁹, O.L. Fedin^{125,o}, W. Fedorko¹⁷¹, S. Feigl¹²¹, L. Feligioni⁸⁸, C. Feng^{36b}, E.J. Feng³², H. Feng⁹², A.B. Fenyuk¹³², L. Feremenga⁸, P. Fernandez Martinez¹⁷⁰, S. Fernandez Perez¹³, J. Ferrando⁴⁵, A. Ferrari¹⁶⁸, P. Ferrari¹⁰⁹, R. Ferrari^{123a}, D.E. Ferreira de Lima^{60b}, A. Ferrer¹⁷⁰, D. Ferrere⁵², C. Ferretti⁹², F. Fiedler⁸⁶, A. Filipčić⁷⁸, M. Filipuzzi⁴⁵, F. Filthaut¹⁰⁸, M. Fincke-Keeler¹⁷², K.D. Finelli¹⁵², M.C.N. Fiolhais^{128a,128c}, L. Fiorini¹⁷⁰, A. Fischer², C. Fischer¹³, J. Fischer¹⁷⁸,

W.C. Fisher⁹³, N. Flaschel⁴⁵, I. Fleck¹⁴³, P. Fleischmann⁹², G.T. Fletcher¹⁴¹,
 R.R.M. Fletcher¹²⁴, T. Flick¹⁷⁸, B.M. Flierl¹⁰², L.R. Flores Castillo^{62a}, M.J. Flowerdew¹⁰³,
 G.T. Forcolin⁸⁷, A. Formica¹³⁸, A. Forti⁸⁷, A.G. Foster¹⁹, D. Fournier¹¹⁹, H. Fox⁷⁵,
 S. Fracchia¹³, P. Francavilla⁸³, M. Franchini^{22a,22b}, D. Francis³², L. Franconi¹²¹, M. Franklin⁵⁹,
 M. Frate¹⁶⁶, M. Fraternali^{123a,123b}, D. Freeborn⁸¹, S.M. Fressard-Batraneanu³², F. Friedrich⁴⁷,
 D. Froidevaux³², J.A. Frost¹²², C. Fukunaga¹⁵⁸, E. Fullana Torregrosa⁸⁶, T. Fusayasu¹⁰⁴,
 J. Fuster¹⁷⁰, C. Gabaldon⁵⁸, O. Gabizon¹⁵⁴, A. Gabrielli^{22a,22b}, A. Gabrielli¹⁶, G.P. Gach^{41a},
 S. Gadatsch³², G. Gagliardi^{53a,53b}, L.G. Gagnon⁹⁷, P. Gagnon⁶⁴, C. Galea¹⁰⁸,
 B. Galhardo^{128a,128c}, E.J. Gallas¹²², B.J. Gallop¹³³, P. Gallus¹³⁰, G. Galster³⁹, K.K. Gan¹¹³,
 S. Ganguly³⁷, J. Gao^{36a}, Y. Gao⁴⁹, Y.S. Gao^{145,g}, F.M. Garay Walls⁴⁹, C. García¹⁷⁰,
 J.E. García Navarro¹⁷⁰, M. Garcia-Sciveres¹⁶, R.W. Gardner³³, N. Garelli¹⁴⁵, V. Garonne¹²¹,
 A. Gascon Bravo⁴⁵, K. Gasnikova⁴⁵, C. Gatti⁵⁰, A. Gaudiello^{53a,53b}, G. Gaudio^{123a},
 L. Gauthier⁹⁷, I.L. Gavrilenko⁹⁸, C. Gay¹⁷¹, G. Gaycken²³, E.N. Gazis¹⁰, Z. Gece¹⁷¹,
 C.N.P. Gee¹³³, Ch. Geich-Gimbel²³, M. Geisen⁸⁶, M.P. Geisler^{60a}, K. Gellerstedt^{148a,148b},
 C. Gemme^{53a}, M.H. Genest⁵⁸, C. Geng^{36a,p}, S. Gentile^{134a,134b}, C. Gentsos¹⁵⁶, S. George⁸⁰,
 D. Gerbaudo¹³, A. Gershon¹⁵⁵, S. Ghasemi¹⁴³, M. Ghneimat²³, B. Giacobbe^{22a},
 S. Giagu^{134a,134b}, P. Giannetti^{126a,126b}, S.M. Gibson⁸⁰, M. Gignac¹⁷¹, M. Gilchriese¹⁶,
 T.P.S. Gillam³⁰, D. Gillberg³¹, G. Gilles¹⁷⁸, D.M. Gingrich^{3,d}, N. Giokaris^{9,*},
 M.P. Giordani^{167a,167c}, F.M. Giorgi^{22a}, P.F. Giraud¹³⁸, P. Giromini⁵⁹, D. Giugni^{94a}, F. Giuli¹²²,
 C. Giuliani¹⁰³, M. Giulini^{60b}, B.K. Gjelsten¹²¹, S. Gkaitatzis¹⁵⁶, I. Gkialas¹⁵⁶,
 E.L. Gkoukousis¹¹⁹, L.K. Gladilin¹⁰¹, C. Glasman⁸⁵, J. Glatzer¹³, P.C.F. Glaysher⁴⁹,
 A. Glazov⁴⁵, M. Goblirsch-Kolb²⁵, J. Godlewski⁴², S. Goldfarb⁹¹, T. Golling⁵², D. Golubkov¹³²,
 A. Gomes^{128a,128b,128d}, R. Gonçalo^{128a}, J. Goncalves Pinto Firmino Da Costa¹³⁸, G. Gonella⁵¹,
 L. Gonella¹⁹, A. Gongadze⁶⁸, S. González de la Hoz¹⁷⁰, S. Gonzalez-Sevilla⁵², L. Goossens³²,
 P.A. Gorbounov⁹⁹, H.A. Gordon²⁷, I. Gorelov¹⁰⁷, B. Gorini³², E. Gorini^{76a,76b}, A. Gorišek⁷⁸,
 E. Gornicki⁴², A.T. Goshaw⁴⁸, C. Gössling⁴⁶, M.I. Gostkin⁶⁸, C.R. Goudet¹¹⁹, D. Goujdami^{137c},
 A.G. Goussiou¹⁴⁰, N. Govender^{147b,q}, E. Gozani¹⁵⁴, L. Graber⁵⁷, I. Grabowska-Bold^{41a},
 P.O.J. Gradin⁵⁸, P. Grafström^{22a,22b}, J. Gramling⁵², E. Gramstad¹²¹, S. Grancagnolo¹⁷,
 V. Gratchev¹²⁵, P.M. Gravila^{28e}, H.M. Gray³², E. Graziani^{136a}, Z.D. Greenwood^{82,r}, C. Grefe²³,
 K. Gregersen⁸¹, I.M. Gregor⁴⁵, P. Grenier¹⁴⁵, K. Grevtsov⁵, J. Griffiths⁸, A.A. Grillo¹³⁹,
 K. Grimm⁷⁵, S. Grinstein^{13,s}, Ph. Gris³⁷, J.-F. Grivaz¹¹⁹, S. Groh⁸⁶, E. Gross¹⁷⁵,
 J. Grosse-Knetter⁵⁷, G.C. Grossi⁸², Z.J. Grout⁸¹, L. Guan⁹², W. Guan¹⁷⁶, J. Guenther⁶⁵,
 F. Guescini⁵², D. Guest¹⁶⁶, O. Gueta¹⁵⁵, B. Gui¹¹³, E. Guido^{53a,53b}, T. Guillemin⁵, S. Guindon²,
 U. Gul⁵⁶, C. Gumpert³², J. Guo^{36c}, Y. Guo^{36a,p}, R. Gupta⁴³, S. Gupta¹²²,
 G. Gustavino^{134a,134b}, P. Gutierrez¹¹⁵, N.G. Gutierrez Ortiz⁸¹, C. Gutsche⁸¹, C. Guyot¹³⁸,
 C. Gwenlan¹²², C.B. Gwilliam⁷⁷, A. Haas¹¹², C. Haber¹⁶, H.K. Hadavand⁸, N. Haddad^{137e},
 A. Hadeef⁸⁸, S. Hageböck²³, M. Hagihara¹⁶⁴, Z. Hajduk⁴², H. Hakobyan^{180,*}, M. Haleem⁴⁵,
 J. Haley¹¹⁶, G. Halladjian⁹³, G.D. Hallewell⁸⁸, K. Hamacher¹⁷⁸, P. Hamal¹¹⁷, K. Hamano¹⁷²,
 A. Hamilton^{147a}, G.N. Hamity¹⁴¹, P.G. Hamnett⁴⁵, L. Han^{36a}, K. Hanagaki^{69,t}, K. Hanawa¹⁵⁷,
 M. Hance¹³⁹, B. Haney¹²⁴, P. Hanke^{60a}, R. Hanna¹³⁸, J.B. Hansen³⁹, J.D. Hansen³⁹,
 M.C. Hansen²³, P.H. Hansen³⁹, K. Hara¹⁶⁴, A.S. Hard¹⁷⁶, T. Harenberg¹⁷⁸, F. Hariri¹¹⁹,
 S. Harkusha⁹⁵, R.D. Harrington⁴⁹, P.F. Harrison¹⁷³, F. Hartjes¹⁰⁹, N.M. Hartmann¹⁰²,
 M. Hasegawa⁷⁰, Y. Hasegawa¹⁴², A. Hasib¹¹⁵, S. Hassani¹³⁸, S. Haug¹⁸, R. Hauser⁹³,
 L. Hauswald⁴⁷, M. Havranek¹²⁹, C.M. Hawkes¹⁹, R.J. Hawkings³², D. Hayakawa¹⁵⁹,
 D. Hayden⁹³, C.P. Hays¹²², J.M. Hays⁷⁹, H.S. Hayward⁷⁷, S.J. Haywood¹³³, S.J. Head¹⁹,
 T. Heck⁸⁶, V. Hedberg⁸⁴, L. Heelan⁸, S. Heim¹²⁴, T. Heim¹⁶, B. Heinemann¹⁶, J.J. Heinrich¹⁰²,
 L. Heinrich¹¹², C. Heinz⁵⁵, J. Hejbal¹²⁹, L. Helary³², S. Hellman^{148a,148b}, C. Helsen³²,
 J. Henderson¹²², R.C.W. Henderson⁷⁵, Y. Heng¹⁷⁶, S. Henkelmann¹⁷¹, A.M. Henriques Correia³²,

S. Henrot-Versille¹¹⁹, G.H. Herbert¹⁷, H. Herde²⁵, V. Herget¹⁷⁷, Y. Hernández Jiménez^{147c},
 G. Herten⁵¹, R. Hertenberger¹⁰², L. Hervas³², G.G. Hesketh⁸¹, N.P. Hessey¹⁰⁹, J.W. Hetherly⁴³,
 E. Higón-Rodríguez¹⁷⁰, E. Hill¹⁷², J.C. Hill³⁰, K.H. Hiller⁴⁵, S.J. Hillier¹⁹, I. Hinchliffe¹⁶,
 E. Hines¹²⁴, R.R. Hinman¹⁶, M. Hirose⁵¹, D. Hirschbuehl¹⁷⁸, X. Hoad⁴⁹, J. Hobbs¹⁵⁰,
 N. Hod^{163a}, M.C. Hodgkinson¹⁴¹, P. Hodgson¹⁴¹, A. Hoecker³², M.R. Hoferkamp¹⁰⁷,
 F. Hoenig¹⁰², D. Hohn²³, T.R. Holmes¹⁶, M. Homann⁴⁶, T. Honda⁶⁹, T.M. Hong¹²⁷,
 B.H. Hooberman¹⁶⁹, W.H. Hopkins¹¹⁸, Y. Horii¹⁰⁵, A.J. Horton¹⁴⁴, J.-Y. Hostachy⁵⁸, S. Hou¹⁵³,
 A. Houmada^{137a}, J. Howarth⁴⁵, J. Hoya⁷⁴, M. Hrabovsky¹¹⁷, I. Hristova¹⁷, J. Hrivnac¹¹⁹,
 T. Hryn'ova⁵, A. Hrynevich⁹⁶, C. Hsu^{147c}, P.J. Hsu⁶³, S.-C. Hsu¹⁴⁰, Q. Hu^{36a}, S. Hu^{36c},
 Y. Huang⁴⁵, Z. Hubacek¹³⁰, F. Hubaut⁸⁸, F. Huegging²³, T.B. Huffman¹²², E.W. Hughes³⁸,
 G. Hughes⁷⁵, M. Huhtinen³², P. Huo¹⁵⁰, N. Huseynov^{68,b}, J. Huston⁹³, J. Huth⁵⁹, G. Iacobucci⁵²,
 G. Iakovidis²⁷, I. Ibragimov¹⁴³, L. Iconomidou-Fayard¹¹⁹, E. Ideal¹⁷⁹, Z. Idrissi^{137e}, P. Iengo³²,
 O. Igonkina^{109,u}, T. Iizawa¹⁷⁴, Y. Ikegami⁶⁹, M. Ikeno⁶⁹, Y. Ilchenko^{11,v}, D. Iliadis¹⁵⁶, N. Ilic¹⁴⁵,
 G. Introzzi^{123a,123b}, P. Ioannou^{9,*}, M. Iodice^{136a}, K. Iordanidou³⁸, V. Ippolito⁵⁹, N. Ishijima¹²⁰,
 M. Ishino¹⁵⁷, M. Ishitsuka¹⁵⁹, R. Ishmukhametov¹¹³, C. Issever¹²², S. Istin^{20a}, F. Ito¹⁶⁴,
 J.M. Iturbe Ponce⁸⁷, R. Iuppa^{162a,162b}, W. Iwanski⁶⁵, H. Iwasaki⁶⁹, J.M. Izen⁴⁴, V. Izzo^{106a},
 S. Jabbar³, B. Jackson¹²⁴, P. Jackson¹, V. Jain², K.B. Jakobi⁸⁶, K. Jakobs⁵¹, S. Jakobsen³²,
 T. Jakoubek¹²⁹, D.O. Jamin¹¹⁶, D.K. Jana⁸², R. Jansky⁶⁵, J. Janssen²³, M. Janus⁵⁷,
 P.A. Janus^{41a}, G. Jarlskog⁸⁴, N. Javadov^{68,b}, T. Javůrek⁵¹, F. Jeanneau¹³⁸, L. Jeanty¹⁶,
 J. Jejelava^{54a,w}, G.-Y. Jeng¹⁵², D. Jennens⁹¹, P. Jenni^{51,x}, C. Jeske¹⁷³, S. Jézéquel⁵, H. Ji¹⁷⁶,
 J. Jia¹⁵⁰, H. Jiang⁶⁷, Y. Jiang^{36a}, Z. Jiang¹⁴⁵, S. Jiggins⁸¹, J. Jimenez Pena¹⁷⁰, S. Jin^{35a},
 A. Jinaru^{28b}, O. Jinnouchi¹⁵⁹, H. Jivan^{147c}, P. Johansson¹⁴¹, K.A. Johns⁷, W.J. Johnson¹⁴⁰,
 K. Jon-And^{148a,148b}, G. Jones¹⁷³, R.W.L. Jones⁷⁵, S. Jones⁷, T.J. Jones⁷⁷, J. Jongmanns^{60a},
 P.M. Jorge^{128a,128b}, J. Jovicevic^{163a}, X. Ju¹⁷⁶, A. Juste Rozas^{13,s}, M.K. Köhler¹⁷⁵,
 A. Kaczmarzka⁴², M. Kado¹¹⁹, H. Kagan¹¹³, M. Kagan¹⁴⁵, S.J. Kahn⁸⁸, T. Kaji¹⁷⁴,
 E. Kajomovitz⁴⁸, C.W. Kalderon¹²², A. Kaluza⁸⁶, S. Kama⁴³, A. Kamenshchikov¹³²,
 N. Kanaya¹⁵⁷, S. Kaneti³⁰, L. Kanjir⁷⁸, V.A. Kantserov¹⁰⁰, J. Kanzaki⁶⁹, B. Kaplan¹¹²,
 L.S. Kaplan¹⁷⁶, A. Kapliy³³, D. Kar^{147c}, K. Karakostas¹⁰, A. Karamaoun³, N. Karastathis¹⁰,
 M.J. Kareem⁵⁷, E. Karentzos¹⁰, M. Karneviy⁸⁶, S.N. Karpov⁶⁸, Z.M. Karpova⁶⁸,
 K. Karthik¹¹², V. Kartvelishvili⁷⁵, A.N. Karyukhin¹³², K. Kasahara¹⁶⁴, L. Kashif¹⁷⁶,
 R.D. Kass¹¹³, A. Kastanas¹⁴⁹, Y. Kataoka¹⁵⁷, C. Kato¹⁵⁷, A. Katre⁵², J. Katzy⁴⁵, K. Kawade¹⁰⁵,
 K. Kawagoe⁷³, T. Kawamoto¹⁵⁷, G. Kawamura⁵⁷, V.F. Kazanin^{111,c}, R. Keeler¹⁷², R. Kehoe⁴³,
 J.S. Keller⁴⁵, J.J. Kempster⁸⁰, H. Keoshkerian¹⁶¹, O. Kepka¹²⁹, B.P. Kerševan⁷⁸, S. Kersten¹⁷⁸,
 R.A. Keyes⁹⁰, M. Khader¹⁶⁹, F. Khalil-zada¹², A. Khanov¹¹⁶, A.G. Kharlamov^{111,c},
 T. Kharlamova^{111,c}, T.J. Khoo⁵², V. Khovanskiy⁹⁹, E. Khramov⁶⁸, J. Khubua^{54b,y}, S. Kido⁷⁰,
 C.R. Kilby⁸⁰, H.Y. Kim⁸, S.H. Kim¹⁶⁴, Y.K. Kim³³, N. Kimura¹⁵⁶, O.M. Kind¹⁷, B.T. King⁷⁷,
 M. King¹⁷⁰, J. Kirk¹³³, A.E. Kiryunin¹⁰³, T. Kishimoto¹⁵⁷, D. Kisielewska^{41a}, F. Kiss⁵¹,
 K. Kiuchi¹⁶⁴, O. Kivernyk¹³⁸, E. Kladiva^{146b}, M.H. Klein³⁸, M. Klein⁷⁷, U. Klein⁷⁷,
 K. Kleinknecht⁸⁶, P. Klimek¹¹⁰, A. Klimentov²⁷, R. Klingenberg⁴⁶, T. Klioutchnikova³²,
 E.-E. Kluge^{60a}, P. Kluit¹⁰⁹, S. Kluth¹⁰³, J. Knapik⁴², E. Kneringer⁶⁵, E.B.F.G. Knoops⁸⁸,
 A. Knue¹⁰³, A. Kobayashi¹⁵⁷, D. Kobayashi¹⁵⁹, T. Kobayashi¹⁵⁷, M. Kobel⁴⁷, M. Kocian¹⁴⁵,
 P. Kodys¹³¹, T. Koffas³¹, E. Koffeman¹⁰⁹, N.M. Köhler¹⁰³, T. Koi¹⁴⁵, H. Kolanoski¹⁷,
 M. Kolb^{60b}, I. Koletsou⁵, A.A. Komar^{98,*}, Y. Komori¹⁵⁷, T. Kondo⁶⁹, N. Kondrashova^{36c},
 K. Köneke⁵¹, A.C. König¹⁰⁸, T. Kono^{69,z}, R. Konoplich^{112,aa}, N. Konstantinidis⁸¹,
 R. Kopeliansky⁶⁴, S. Koperny^{41a}, L. Köpke⁸⁶, A.K. Kopp⁵¹, K. Korcyl⁴², K. Kordas¹⁵⁶,
 A. Korn⁸¹, A.A. Korol^{111,c}, I. Korolkov¹³, E.V. Korolkova¹⁴¹, O. Kortner¹⁰³, S. Kortner¹⁰³,
 T. Kosek¹³¹, V.V. Kostyukhin²³, A. Kotwal⁴⁸, A. Koulouris¹⁰,
 A. Kourkouveli-Charalampidi^{123a,123b}, C. Kourkouvelis⁹, V. Kouskoura²⁷, A.B. Kowalewska⁴²,

R. Kowalewski¹⁷², T.Z. Kowalski^{41a}, C. Kozakai¹⁵⁷, W. Kozanecki¹³⁸, A.S. Kozhin¹³², V.A. Kramarenko¹⁰¹, G. Kramberger⁷⁸, D. Krasnopevtsev¹⁰⁰, M.W. Krasny⁸³, A. Krasznahorkay³², A. Kravchenko²⁷, M. Kretz^{60c}, J. Kretzschmar⁷⁷, K. Kreutzfeldt⁵⁵, P. Krieger¹⁶¹, K. Krizka³³, K. Kroeninger⁴⁶, H. Kroha¹⁰³, J. Kroll¹²⁴, J. Kroseberg²³, J. Krstic¹⁴, U. Kruchonak⁶⁸, H. Krüger²³, N. Krumnack⁶⁷, M.C. Kruse⁴⁸, M. Kruskal²⁴, T. Kubota⁹¹, H. Kucuk⁸¹, S. Kuday^{4b}, J.T. Kuechler¹⁷⁸, S. Kuehn⁵¹, A. Kugel^{60c}, F. Kuger¹⁷⁷, T. Kuhl⁴⁵, V. Kukhtin⁶⁸, R. Kukla¹³⁸, Y. Kulchitsky⁹⁵, S. Kuleshov^{34b}, M. Kuna^{134a,134b}, T. Kunigo⁷¹, A. Kupco¹²⁹, H. Kurashige⁷⁰, Y.A. Kurochkin⁹⁵, M.G. Kurth⁴⁴, V. Kus¹²⁹, E.S. Kuwertz¹⁷², M. Kuze¹⁵⁹, J. Kvita¹¹⁷, T. Kwan¹⁷², D. Kyriazopoulos¹⁴¹, A. La Rosa¹⁰³, J.L. La Rosa Navarro^{26d}, L. La Rotonda^{40a,40b}, C. Lacasta¹⁷⁰, F. Lacava^{134a,134b}, J. Lacey³¹, H. Lacker¹⁷, D. Lacour⁸³, V.R. Lacuesta¹⁷⁰, E. Ladygin⁶⁸, R. Lafaye⁵, B. Laforge⁸³, T. Lagouri¹⁷⁹, S. Lai⁵⁷, S. Lammers⁶⁴, W. Lampl⁷, E. Lançon¹³⁸, U. Landgraf⁵¹, M.P.J. Landon⁷⁹, M.C. Lanfermann⁵², V.S. Lang^{60a}, J.C. Lange¹³, A.J. Lankford¹⁶⁶, F. Lanni²⁷, K. Lantzsch²³, A. Lanza^{123a}, S. Laplace⁸³, C. Lapoire³², J.F. Laporte¹³⁸, T. Lari^{94a}, F. Lasagni Manghi^{22a,22b}, M. Lassnig³², P. Laurelli⁵⁰, W. Lavrijsen¹⁶, A.T. Law¹³⁹, P. Laycock⁷⁷, T. Lazovich⁵⁹, M. Lazzaroni^{94a,94b}, B. Le⁹¹, O. Le Dortz⁸³, E. Le Guirriec⁸⁸, E.P. Le Quilleuc¹³⁸, M. LeBlanc¹⁷², T. LeCompte⁶, F. Ledroit-Guillon⁵⁸, C.A. Lee²⁷, S.C. Lee¹⁵³, L. Lee¹, B. Lefebvre⁹⁰, G. Lefebvre⁸³, M. Lefebvre¹⁷², F. Legger¹⁰², C. Leggett¹⁶, A. Lehan⁷⁷, G. Lehmann Miotto³², X. Lei⁷, W.A. Leight³¹, A.G. Leister¹⁷⁹, M.A.L. Leite^{26d}, R. Leitner¹³¹, D. Lellouch¹⁷⁵, B. Lemmer⁵⁷, K.J.C. Leney⁸¹, T. Lenz²³, B. Lenzi³², R. Leone⁷, S. Leone^{126a,126b}, C. Leonidopoulos⁴⁹, S. Leontsinis¹⁰, G. Lerner¹⁵¹, C. Leroy⁹⁷, A.A.J. Lesage¹³⁸, C.G. Lester³⁰, M. Levchenko¹²⁵, J. Levêque⁵, D. Levin⁹², L.J. Levinson¹⁷⁵, M. Levy¹⁹, D. Lewis⁷⁹, A.M. Leyko²³, M. Leyton⁴⁴, B. Li^{36a,p}, C. Li^{36a}, H. Li¹⁵⁰, L. Li⁴⁸, L. Li^{36c}, Q. Li^{35a}, S. Li⁴⁸, X. Li⁸⁷, Y. Li¹⁴³, Z. Liang^{35a}, B. Liberti^{135a}, A. Liblong¹⁶¹, P. Lichard³², K. Lie¹⁶⁹, J. Liebal²³, W. Liebig¹⁵, A. Limosani¹⁵², S.C. Lin^{153,ab}, T.H. Lin⁸⁶, B.E. Lindquist¹⁵⁰, A.E. Lioni⁵², E. Lipeles¹²⁴, A. Lipniacka¹⁵, M. Lisovyi^{60b}, T.M. Liss¹⁶⁹, A. Lister¹⁷¹, A.M. Litke¹³⁹, B. Liu^{153,ac}, D. Liu¹⁵³, H. Liu⁹², H. Liu²⁷, J. Liu^{36b}, J.B. Liu^{36a}, K. Liu⁸⁸, L. Liu¹⁶⁹, M. Liu^{36a}, Y.L. Liu^{36a}, Y. Liu^{36a}, M. Livan^{123a,123b}, A. Lleres⁵⁸, J. Llorente Merino^{35a}, S.L. Lloyd⁷⁹, F. Lo Sterzo¹⁵³, E.M. Lobodzinska⁴⁵, P. Loch⁷, F.K. Loebinger⁸⁷, K.M. Loew²⁵, A. Loginov^{179,*}, T. Lohse¹⁷, K. Lohwasser⁴⁵, M. Lokajicek¹²⁹, B.A. Long²⁴, J.D. Long¹⁶⁹, R.E. Long⁷⁵, L. Longo^{76a,76b}, K.A. Looper¹¹³, J.A. Lopez Lopez^{34b}, D. Lopez Mateos⁵⁹, B. Lopez Paredes¹⁴¹, I. Lopez Paz¹³, A. Lopez Solis⁸³, J. Lorenz¹⁰², N. Lorenzo Martinez⁶⁴, M. Losada²¹, P.J. Lösel¹⁰², X. Lou^{35a}, A. Lounis¹¹⁹, J. Love⁶, P.A. Love⁷⁵, H. Lu^{62a}, N. Lu⁹², H.J. Lubatti¹⁴⁰, C. Luci^{134a,134b}, A. Lucotte⁵⁸, C. Luedtke⁵¹, F. Luehring⁶⁴, W. Lukas⁶⁵, L. Luminari^{134a}, O. Lundberg^{148a,148b}, B. Lund-Jensen¹⁴⁹, P.M. Luzi⁸³, D. Lynn²⁷, R. Lysak¹²⁹, E. Lytken⁸⁴, V. Lyubushkin⁶⁸, H. Ma²⁷, L.L. Ma^{36b}, Y. Ma^{36b}, G. Maccarrone⁵⁰, A. Macchiolo¹⁰³, C.M. Macdonald¹⁴¹, B. Maček⁷⁸, J. Machado Miguens^{124,128b}, D. Madaffari⁸⁸, R. Madar³⁷, H.J. Maddocks¹⁶⁸, W.F. Mader⁴⁷, A. Madsen⁴⁵, J. Maeda⁷⁰, S. Maeland¹⁵, T. Maeno²⁷, A. Maevskiy¹⁰¹, E. Magradze⁵⁷, J. Mahlstedt¹⁰⁹, C. Maiani¹¹⁹, C. Maidantchik^{26a}, A.A. Maier¹⁰³, T. Maier¹⁰², A. Maio^{128a,128b,128d}, S. Majewski¹¹⁸, Y. Makida⁶⁹, N. Makovec¹¹⁹, B. Malaescu⁸³, Pa. Malecki⁴², V.P. Maleev¹²⁵, F. Malek⁵⁸, U. Mallik⁶⁶, D. Malon⁶, C. Malone¹⁴⁵, C. Malone³⁰, S. Maltezos¹⁰, S. Mal'ukov³², J. Mamuzic¹⁷⁰, G. Mancini⁵⁰, L. Mandelli^{94a}, I. Mandić⁷⁸, J. Maneira^{128a,128b}, L. Manhaes de Andrade Filho^{26b}, J. Manjarres Ramos^{163b}, A. Mann¹⁰², A. Manousos³², B. Mansoulie¹³⁸, J.D. Mansour^{35a}, R. Mantifel⁹⁰, M. Mantoani⁵⁷, S. Manzoni^{94a,94b}, L. Mapelli³², G. Marceca²⁹, L. March⁵², G. Marchiori⁸³, M. Marcisovsky¹²⁹, M. Marjanovic¹⁴, D.E. Marley⁹², F. Marroquim^{26a}, S.P. Marsden⁸⁷, Z. Marshall¹⁶, S. Marti-Garcia¹⁷⁰, B. Martin⁹³, T.A. Martin¹⁷³, V.J. Martin⁴⁹, B. Martin dit Latour¹⁵,

M. Martinez^{13,s}, V.I. Martinez Outschoorn¹⁶⁹, S. Martin-Haugh¹³³, V.S. Martoiu^{28b},
 A.C. Martyniuk⁸¹, A. Marzin³², L. Masetti⁸⁶, T. Mashimo¹⁵⁷, R. Mashinistov⁹⁸, J. Masik⁸⁷,
 A.L. Maslennikov^{111,c}, I. Massa^{22a,22b}, L. Massa^{22a,22b}, P. Mastrandrea⁵,
 A. Mastroberardino^{40a,40b}, T. Masubuchi¹⁵⁷, P. Mättig¹⁷⁸, J. Mattmann⁸⁶, J. Maurer^{28b},
 S.J. Maxfield⁷⁷, D.A. Maximov^{111,c}, R. Mazini¹⁵³, I. Maznas¹⁵⁶, S.M. Mazza^{94a,94b},
 N.C. Mc Fadden¹⁰⁷, G. Mc Goldrick¹⁶¹, S.P. Mc Kee⁹², A. McCarn⁹², R.L. McCarthy¹⁵⁰,
 T.G. McCarthy¹⁰³, L.I. McClymont⁸¹, E.F. McDonald⁹¹, J.A. McFayden⁸¹, G. Mchedlidze⁵⁷,
 S.J. McMahon¹³³, R.A. McPherson^{172,m}, M. Medinnis⁴⁵, S. Meehan¹⁴⁰, S. Mehlhase¹⁰²,
 A. Mehta⁷⁷, K. Meier^{60a}, C. Meineck¹⁰², B. Meirose⁴⁴, D. Melini¹⁷⁰, B.R. Mellado Garcia^{147c},
 M. Melo^{146a}, F. Meloni¹⁸, L. Meng⁷⁷, X.T. Meng⁹², A. Mengarelli^{22a,22b}, S. Menke¹⁰³,
 E. Meoni¹⁶⁵, S. Mergelmeyer¹⁷, P. Mermod⁵², L. Merola^{106a,106b}, C. Meroni^{94a}, F.S. Merritt³³,
 A. Messina^{134a,134b}, J. Metcalfe⁶, A.S. Mete¹⁶⁶, C. Meyer⁸⁶, C. Meyer¹²⁴, J-P. Meyer¹³⁸,
 J. Meyer¹⁰⁹, H. Meyer Zu Theenhausen^{60a}, F. Miano¹⁵¹, R.P. Middleton¹³³, S. Miglioranzi^{53a,53b},
 L. Mijović⁴⁹, G. Mikenberg¹⁷⁵, M. Mikestikova¹²⁹, M. Mikuz⁷⁸, M. Milesi⁹¹, A. Milic²⁷,
 D.W. Miller³³, C. Mills⁴⁹, A. Milov¹⁷⁵, D.A. Milstead^{148a,148b}, A.A. Minaenko¹³², Y. Minami¹⁵⁷,
 I.A. Minashvili⁶⁸, A.I. Mincer¹¹², B. Mindur^{41a}, M. Mineev⁶⁸, Y. Minegishi¹⁵⁷, Y. Ming¹⁷⁶,
 L.M. Mir¹³, K.P. Mistry¹²⁴, T. Mitani¹⁷⁴, J. Mitrevski¹⁰², V.A. Mitsou¹⁷⁰, A. Miucci¹⁸,
 P.S. Miyagawa¹⁴¹, A. Mizukami⁶⁹, J.U. Mjörnmark⁸⁴, M. Mlynarikova¹³¹, T. Moa^{148a,148b},
 K. Mochizuki⁹⁷, P. Mogg⁵¹, S. Mohapatra³⁸, S. Molander^{148a,148b}, R. Moles-Valls²³,
 R. Monden⁷¹, M.C. Mondragon⁹³, K. Mönig⁴⁵, J. Monk³⁹, E. Monnier⁸⁸, A. Montalbano¹⁵⁰,
 J. Montejo Berlingen³², F. Monticelli⁷⁴, S. Monzani^{94a,94b}, R.W. Moore³, N. Morange¹¹⁹,
 D. Moreno²¹, M. Moreno Llácer⁵⁷, P. Morettini^{53a}, S. Morgenstern³², D. Mori¹⁴⁴, T. Mori¹⁵⁷,
 M. Morii⁵⁹, M. Morinaga¹⁵⁷, V. Morisbak¹²¹, S. Moritz⁸⁶, A.K. Morley¹⁵², G. Mornacchi³²,
 J.D. Morris⁷⁹, S.S. Mortensen³⁹, L. Morvaj¹⁵⁰, M. Mosidze^{54b}, H.J. Moss¹⁴¹, J. Moss^{145,ad},
 K. Motohashi¹⁵⁹, R. Mount¹⁴⁵, E. Mountricha²⁷, E.J.W. Moyse⁸⁹, S. Muanza⁸⁸, R.D. Mudd¹⁹,
 F. Mueller¹⁰³, J. Mueller¹²⁷, R.S.P. Mueller¹⁰², T. Mueller³⁰, D. Muenstermann⁷⁵, P. Mullen⁵⁶,
 G.A. Mullier¹⁸, F.J. Munoz Sanchez⁸⁷, J.A. Murillo Quijada¹⁹, W.J. Murray^{173,133},
 H. Mushheghyan⁵⁷, M. Muškinja⁷⁸, A.G. Myagkov^{132,ae}, M. Myska¹³⁰, B.P. Nachman¹⁴⁵,
 O. Nackenhurst⁵², K. Nagai¹²², R. Nagai^{69,z}, K. Nagano⁶⁹, Y. Nagasaka⁶¹, K. Nagata¹⁶⁴,
 M. Nagel⁵¹, E. Nagy⁸⁸, A.M. Nairz³², Y. Nakahama¹⁰⁵, K. Nakamura⁶⁹, T. Nakamura¹⁵⁷,
 I. Nakano¹¹⁴, R.F. Naranjo Garcia⁴⁵, R. Narayan¹¹, D.I. Narrias Villar^{60a}, I. Naryshkin¹²⁵,
 T. Naumann⁴⁵, G. Navarro²¹, R. Nayyar⁷, H.A. Neal⁹², P.Yu. Nechaeva⁹⁸, T.J. Neep⁸⁷,
 A. Negri^{123a,123b}, M. Negrini^{22a}, S. Nektarijevic¹⁰⁸, C. Nellist¹¹⁹, A. Nelson¹⁶⁶, S. Nemecek¹²⁹,
 P. Nemethy¹¹², A.A. Nepomuceno^{26a}, M. Nessi^{32,af}, M.S. Neubauer¹⁶⁹, M. Neumann¹⁷⁸,
 R.M. Neves¹¹², P. Nevski²⁷, P.R. Newman¹⁹, D.H. Nguyen⁶, T. Nguyen Manh⁹⁷,
 R.B. Nickerson¹²², R. Nicolaidou¹³⁸, J. Nielsen¹³⁹, A. Nikiforov¹⁷, V. Nikolaenko^{132,ae},
 I. Nikolic-Audit⁸³, K. Nikolopoulos¹⁹, J.K. Nilsen¹²¹, P. Nilsson²⁷, Y. Ninomiya¹⁵⁷, A. Nisati^{134a},
 R. Nisius¹⁰³, T. Nobe¹⁵⁷, M. Nomachi¹²⁰, I. Nomidis³¹, T. Nooney⁷⁹, S. Norberg¹¹⁵,
 M. Nordberg³², N. Norjoharuddeen¹²², O. Novgorodova⁴⁷, S. Nowak¹⁰³, M. Nozaki⁶⁹,
 L. Nozka¹¹⁷, K. Ntekas¹⁶⁶, E. Nurse⁸¹, F. Nuti⁹¹, F. O'grady⁷, D.C. O'Neil¹⁴⁴, A.A. O'Rourke⁴⁵,
 V. O'Shea⁵⁶, F.G. Oakham^{31,d}, H. Oberlack¹⁰³, T. Obermann²³, J. Ocariz⁸³, A. Ochi⁷⁰,
 I. Ochoa³⁸, J.P. Ochoa-Ricoux^{34a}, S. Oda⁷³, S. Odaka⁶⁹, H. Ogren⁶⁴, A. Oh⁸⁷, S.H. Oh⁴⁸,
 C.C. Ohm¹⁶, H. Ohman¹⁶⁸, H. Oide^{53a,53b}, H. Okawa¹⁶⁴, Y. Okumura¹⁵⁷, T. Okuyama⁶⁹,
 A. Olariu^{28b}, L.F. Oleiro Seabra^{128a}, S.A. Olivares Pino⁴⁹, D. Oliveira Damazio²⁷,
 A. Olszewski⁴², J. Olszowska⁴², A. Onofre^{128a,128e}, K. Onogi¹⁰⁵, P.U.E. Onyisi^{11,v},
 M.J. Oreglia³³, Y. Oren¹⁵⁵, D. Orestano^{136a,136b}, N. Orlando^{62b}, R.S. Orr¹⁶¹,
 B. Osculati^{53a,53b,*}, R. Ospanov⁸⁷, G. Otero y Garzon²⁹, H. Otono⁷³, M. Ouchrif^{137d},
 F. Ould-Saada¹²¹, A. Ouraou¹³⁸, K.P. Oussoren¹⁰⁹, Q. Ouyang^{35a}, M. Owen⁵⁶, R.E. Owen¹⁹,

V.E. Ozcan^{20a}, N. Ozturk⁸, K. Pachal¹⁴⁴, A. Pacheco Pages¹³, L. Pacheco Rodriguez¹³⁸,
C. Padilla Aranda¹³, M. Pagáčová⁵¹, S. Pagan Griso¹⁶, M. Paganini¹⁷⁹, F. Paige²⁷, P. Pais⁸⁹,
K. Pajchel¹²¹, G. Palacino⁶⁴, S. Palazzo^{40a,40b}, S. Palestini³², M. Palka^{41b}, D. Pallin³⁷,
E.St. Panagiotopoulou¹⁰, I. Panagoulas¹⁰, C.E. Pandini⁸³, J.G. Panduro Vazquez⁸⁰,
P. Pani^{148a,148b}, S. Panitkin²⁷, D. Pantea^{28b}, L. Paolozzi⁵², Th.D. Papadopoulou¹⁰,
K. Papageorgiou¹⁵⁶, A. Paramonov⁶, D. Paredes Hernandez¹⁷⁹, A.J. Parker⁷⁵, M.A. Parker³⁰,
K.A. Parker¹⁴¹, F. Parodi^{53a,53b}, J.A. Parsons³⁸, U. Parzefall⁵¹, V.R. Pascuzzi¹⁶¹,
E. Pasqualucci^{134a}, S. Passaggio^{53a}, Fr. Pastore⁸⁰, G. Pásztor^{31,ag}, S. Pataria¹⁷⁸, J.R. Pater⁸⁷,
T. Pauly³², J. Pearce¹⁷², B. Pearson¹¹⁵, L.E. Pedersen³⁹, M. Pedersen¹²¹, S. Pedraza Lopez¹⁷⁰,
R. Pedro^{128a,128b}, S.V. Peleganchuk^{111,c}, O. Penc¹²⁹, C. Peng^{35a}, H. Peng^{36a}, J. Penwell⁶⁴,
B.S. Peralva^{26b}, M.M. Perego¹³⁸, D.V. Perepelitsa²⁷, E. Perez Codina^{163a}, L. Perini^{94a,94b},
H. Pernegger³², S. Perrella^{106a,106b}, R. Peschke⁴⁵, V.D. Peshekhonov⁶⁸, K. Peters⁴⁵,
R.F.Y. Peters⁸⁷, B.A. Petersen³², T.C. Petersen³⁹, E. Petit⁵⁸, A. Petridis¹, C. Petridou¹⁵⁶,
P. Petroff¹¹⁹, E. Petrolo^{134a}, M. Petrov¹²², F. Petrucci^{136a,136b}, N.E. Pettersson⁸⁹, A. Peyaud¹³⁸,
R. Pezoa^{34b}, P.W. Phillips¹³³, G. Piacquadio^{145,ah}, E. Pianori¹⁷³, A. Picazio⁸⁹, E. Piccaro⁷⁹,
M. Piccinini^{22a,22b}, M.A. Pickering¹²², R. Piegai²⁹, J.E. Pilcher³³, A.D. Pilkington⁸⁷,
A.W.J. Pin⁸⁷, M. Pinamonti^{167a,167c,ai}, J.L. Pinfold³, A. Pingel³⁹, S. Pires⁸³, H. Pirumov⁴⁵,
M. Pitt¹⁷⁵, L. Plazak^{146a}, M.-A. Pleier²⁷, V. Pleskot⁸⁶, E. Plotnikova⁶⁸, D. Pluth⁶⁷,
R. Poettgen^{148a,148b}, L. Poggioli¹¹⁹, D. Pohl²³, G. Polesello^{123a}, A. Poley⁴⁵, A. Policicchio^{40a,40b},
R. Polifka¹⁶¹, A. Polini^{22a}, C.S. Pollard⁵⁶, V. Polychronakos²⁷, K. Pommès³², L. Pontecorvo^{134a},
B.G. Pope⁹³, G.A. Popeneciu^{28c}, A. Poppleton³², S. Pospisil¹³⁰, K. Potamianos¹⁶, I.N. Potrap⁶⁸,
C.J. Potter³⁰, C.T. Potter¹¹⁸, G. Poulard³², J. Poveda³², V. Pozdnyakov⁶⁸,
M.E. Pozo Astigarraga³², P. Pralavorio⁸⁸, A. Pranko¹⁶, S. Prell⁶⁷, D. Price⁸⁷, L.E. Price⁶,
M. Primavera^{76a}, S. Prince⁹⁰, K. Prokofiev^{62c}, F. Prokoshin^{34b}, S. Protopopescu²⁷,
J. Proudfoot⁶, M. Przybycien^{41a}, D. Puddu^{136a,136b}, M. Purohit^{27,aj}, P. Puzo¹¹⁹, J. Qian⁹²,
G. Qin⁵⁶, Y. Qin⁸⁷, A. Quadt⁵⁷, W.B. Quayle^{167a,167b}, M. Queitsch-Maitland⁴⁵, D. Quilty⁵⁶,
S. Raddum¹²¹, V. Radeka²⁷, V. Radescu¹²², S.K. Radhakrishnan¹⁵⁰, P. Radloff¹¹⁸, P. Rados⁹¹,
F. Ragusa^{94a,94b}, G. Rahal¹⁸¹, J.A. Raine⁸⁷, S. Rajagopalan²⁷, M. Rammensee³²,
C. Rangel-Smith¹⁶⁸, M.G. Ratti^{94a,94b}, D.M. Rauch⁴⁵, F. Rauscher¹⁰², S. Rave⁸⁶,
T. Ravenscroft⁵⁶, I. Ravinovich¹⁷⁵, M. Raymond³², A.L. Read¹²¹, N.P. Readioff⁷⁷,
M. Reale^{76a,76b}, D.M. Rebuffi^{123a,123b}, A. Redelbach¹⁷⁷, G. Redlinger²⁷, R. Reece¹³⁹,
R.G. Reed^{147c}, K. Reeves⁴⁴, L. Rehnisch¹⁷, J. Reichert¹²⁴, A. Reiss⁸⁶, C. Rembser³², H. Ren^{35a},
M. Rescigno^{134a}, S. Resconi^{94a}, O.L. Rezanova^{111,c}, P. Reznicek¹³¹, R. Rezvani⁹⁷, R. Richter¹⁰³,
S. Richter⁸¹, E. Richter-Was^{41b}, O. Ricken²³, M. Ridel⁸³, P. Rieck¹⁷, C.J. Riegel¹⁷⁸, J. Rieger⁵⁷,
O. Rifki¹¹⁵, M. Rijssenbeek¹⁵⁰, A. Rimoldi^{123a,123b}, M. Rimoldi¹⁸, L. Rinaldi^{22a}, B. Ristić⁵²,
E. Ritsch³², I. Riu¹³, F. Rizatdinova¹¹⁶, E. Rizvi⁷⁹, C. Rizzi¹³, S.H. Robertson^{90,m},
A. Robichaud-Veronneau⁹⁰, D. Robinson³⁰, J.E.M. Robinson⁴⁵, A. Robson⁵⁶, C. Roda^{126a,126b},
Y. Rodina^{88,ak}, A. Rodriguez Perez¹³, D. Rodriguez Rodriguez¹⁷⁰, S. Roe³², C.S. Rogan⁵⁹,
O. Røhne¹²¹, J. Roloff⁵⁹, A. Romaniouk¹⁰⁰, M. Romano^{22a,22b}, S.M. Romano Saez³⁷,
E. Romero Adam¹⁷⁰, N. Rompotis¹⁴⁰, M. Ronzani⁵¹, L. Roos⁸³, E. Ros¹⁷⁰, S. Rosati^{134a},
K. Rosbach⁵¹, P. Rose¹³⁹, N.-A. Rosien⁵⁷, V. Rossetti^{148a,148b}, E. Rossi^{106a,106b}, L.P. Rossi^{53a},
J.H.N. Rosten³⁰, R. Rosten¹⁴⁰, M. Rotaru^{28b}, I. Roth¹⁷⁵, J. Rothberg¹⁴⁰, D. Rousseau¹¹⁹,
A. Rozanov⁸⁸, Y. Rozen¹⁵⁴, X. Ruan^{147c}, F. Rubbo¹⁴⁵, M.S. Rudolph¹⁶¹, F. Rühr⁵¹,
A. Ruiz-Martinez³¹, Z. Rurikova⁵¹, N.A. Rusakovich⁶⁸, A. Ruschke¹⁰², H.L. Russell¹⁴⁰,
J.P. Rutherford⁷, N. Ruthmann³², Y.F. Ryabov¹²⁵, M. Rybar¹⁶⁹, G. Rybkin¹¹⁹, S. Ryu⁶,
A. Ryzhov¹³², G.F. Rzehorz⁵⁷, A.F. Saavedra¹⁵², G. Sabato¹⁰⁹, S. Sacerdoti²⁹,
H.F.W. Sadrozinski¹³⁹, R. Sadykov⁶⁸, F. Safai Tehrani^{134a}, P. Saha¹¹⁰, M. Sahinsoy^{60a},
M. Saimpert¹³⁸, T. Saito¹⁵⁷, H. Sakamoto¹⁵⁷, Y. Sakurai¹⁷⁴, G. Salamanna^{136a,136b},

A. Salamon^{135a,135b}, J.E. Salazar Loyola^{34b}, D. Salek¹⁰⁹, P.H. Sales De Bruin¹⁴⁰, D. Salihagic¹⁰³,
 A. Salnikov¹⁴⁵, J. Salt¹⁷⁰, D. Salvatore^{40a,40b}, F. Salvatore¹⁵¹, A. Salvucci^{62a,62b,62c},
 A. Salzburger³², D. Sammel⁵¹, D. Sampsonidis¹⁵⁶, J. Sánchez¹⁷⁰, V. Sanchez Martinez¹⁷⁰,
 A. Sanchez Pineda^{106a,106b}, H. Sandaker¹²¹, R.L. Sandbach⁷⁹, M. Sandhoff¹⁷⁸, C. Sandoval²¹,
 D.P.C. Sankey¹³³, M. Sannino^{53a,53b}, A. Sansoni⁵⁰, C. Santoni³⁷, R. Santonico^{135a,135b},
 H. Santos^{128a}, I. Santoyo Castillo¹⁵¹, K. Sapp¹²⁷, A. Saponov⁶⁸, J.G. Saraiva^{128a,128d},
 B. Sarrazin²³, O. Sasaki⁶⁹, K. Sato¹⁶⁴, E. Sauvan⁵, G. Savage⁸⁰, P. Savard^{161,d}, N. Savic¹⁰³,
 C. Sawyer¹³³, L. Sawyer^{82,r}, J. Saxon³³, C. Sbarra^{22a}, A. Sbrizzi^{22a,22b}, T. Scanlon⁸¹,
 D.A. Scannicchio¹⁶⁶, M. Scarcella¹⁵², V. Scarfone^{40a,40b}, J. Schaarschmidt¹⁷⁵, P. Schacht¹⁰³,
 B.M. Schachtner¹⁰², D. Schaefer³², L. Schaefer¹²⁴, R. Schaefer⁴⁵, J. Schaeffer⁸⁶, S. Schaepe²³,
 S. Schaetzel^{60b}, U. Schäfer⁸⁶, A.C. Schaffer¹¹⁹, D. Schaile¹⁰², R.D. Schamberger¹⁵⁰, V. Scharf^{60a},
 V.A. Schegelsky¹²⁵, D. Scheirich¹³¹, M. Schernau¹⁶⁶, C. Schiavi^{53a,53b}, S. Schier¹³⁹, C. Schillo⁵¹,
 M. Schioppa^{40a,40b}, S. Schlenker³², K.R. Schmidt-Sommerfeld¹⁰³, K. Schmieden³², C. Schmitt⁸⁶,
 S. Schmitt⁴⁵, S. Schmitz⁸⁶, B. Schneider^{163a}, U. Schnoor⁵¹, L. Schoeffel¹³⁸, A. Schoening^{60b},
 B.D. Schoenrock⁹³, E. Schopf²³, M. Schott⁸⁶, J.F.P. Schouwenberg¹⁰⁸, J. Schovancova⁸,
 S. Schramm⁵², M. Schreyer¹⁷⁷, N. Schuh⁸⁶, A. Schulte⁸⁶, M.J. Schultens²³,
 H.-C. Schultz-Coulon^{60a}, H. Schulz¹⁷, M. Schumacher⁵¹, B.A. Schumm¹³⁹, Ph. Schune¹³⁸,
 A. Schwartzman¹⁴⁵, T.A. Schwarz⁹², H. Schweiger⁸⁷, Ph. Schwemling¹³⁸, R. Schwienhorst⁹³,
 J. Schwindling¹³⁸, T. Schwindt²³, G. Sciolla²⁵, F. Scuri^{126a,126b}, F. Scutti⁹¹, J. Searcy⁹²,
 P. Seema²³, S.C. Seidel¹⁰⁷, A. Seiden¹³⁹, F. Seifert¹³⁰, J.M. Seixas^{26a}, G. Sekhniaidze^{106a},
 K. Sekhon⁹², S.J. Sekula⁴³, D.M. Seliverstov^{125,*}, N. Semprini-Cesari^{22a,22b}, C. Serfon¹²¹,
 L. Serin¹¹⁹, L. Serkin^{167a,167b}, M. Sessa^{136a,136b}, R. Seuster¹⁷², H. Severini¹¹⁵, T. Sfiligoi⁷⁸,
 F. Sforza³², A. Sfyrla⁵², E. Shabalina⁵⁷, N.W. Shaikh^{148a,148b}, L.Y. Shan^{35a}, R. Shang¹⁶⁹,
 J.T. Shank²⁴, M. Shapiro¹⁶, P.B. Shatalov⁹⁹, K. Shaw^{167a,167b}, S.M. Shaw⁸⁷,
 A. Shcherbakova^{148a,148b}, C.Y. Shehu¹⁵¹, P. Sherwood⁸¹, L. Shi^{153,al}, S. Shimizu⁷⁰,
 C.O. Shimmmin¹⁶⁶, M. Shimojima¹⁰⁴, S. Shirabe⁷³, M. Shiyakova^{68,am}, A. Shmeleva⁹⁸,
 D. Shoaleh Saadi⁹⁷, M.J. Shochet³³, S. Shojaii^{94a}, D.R. Shope¹¹⁵, S. Shrestha¹¹³, E. Shulga¹⁰⁰,
 M.A. Shupe⁷, P. Sicho¹²⁹, A.M. Sickles¹⁶⁹, P.E. Sidebo¹⁴⁹, E. Sideras Haddad^{147c},
 O. Sidiropoulou¹⁷⁷, D. Sidorov¹¹⁶, A. Sidoti^{22a,22b}, F. Siegert⁴⁷, Dj. Sijacki¹⁴, J. Silva^{128a,128d},
 S.B. Silverstein^{148a}, V. Simak¹³⁰, Lj. Simic¹⁴, S. Simion¹¹⁹, E. Simioni⁸⁶, B. Simmons⁸¹,
 D. Simon³⁷, M. Simon⁸⁶, P. Sinervo¹⁶¹, N.B. Sinev¹¹⁸, M. Sioli^{22a,22b}, G. Siragusa¹⁷⁷,
 S.Yu. Sivoklov¹⁰¹, J. Sjölin^{148a,148b}, M.B. Skinner⁷⁵, H.P. Skottowe⁵⁹, P. Skubic¹¹⁵,
 M. Slater¹⁹, T. Slavicek¹³⁰, M. Slawinska¹⁰⁹, K. Sliwa¹⁶⁵, R. Slovak¹³¹, V. Smakhtin¹⁷⁵,
 B.H. Smart⁵, L. Smestad¹⁵, J. Smiesko^{146a}, S.Yu. Smirnov¹⁰⁰, Y. Smirnov¹⁰⁰,
 L.N. Smirnova^{101,an}, O. Smirnova⁸⁴, J.W. Smith⁵⁷, M.N.K. Smith³⁸, R.W. Smith³⁸,
 M. Smizanska⁷⁵, K. Smolek¹³⁰, A.A. Snesarev⁹⁸, I.M. Snyder¹¹⁸, S. Snyder²⁷, R. Sobie^{172,m},
 F. Socher⁴⁷, A. Soffer¹⁵⁵, D.A. Soh¹⁵³, G. Sokhrannyi⁷⁸, C.A. Solans Sanchez³², M. Solar¹³⁰,
 E.Yu. Soldatov¹⁰⁰, U. Soldevila¹⁷⁰, A.A. Solodkov¹³², A. Soloshenko⁶⁸, O.V. Solovyanov¹³²,
 V. Solovyev¹²⁵, P. Sommer⁵¹, H. Son¹⁶⁵, H.Y. Song^{36a,ao}, A. Sood¹⁶, A. Sopczak¹³⁰, V. Sopko¹³⁰,
 V. Sorin¹³, D. Sosa^{60b}, C.L. Sotiropoulou^{126a,126b}, R. Soualah^{167a,167c}, A.M. Soukharev^{111,c},
 D. South⁴⁵, B.C. Sowden⁸⁰, S. Spagnolo^{76a,76b}, M. Spalla^{126a,126b}, M. Spangenberg¹⁷³,
 F. Spanò⁸⁰, D. Sperlich¹⁷, F. Spettel¹⁰³, R. Spighi^{22a}, G. Spigo³², L.A. Spiller⁹¹, M. Spousta¹³¹,
 R.D. St. Denis^{56,*}, A. Stabile^{94a}, R. Stamen^{60a}, S. Stamm¹⁷, E. Stanecka⁴², R.W. Stanek⁶,
 C. Stanescu^{136a}, M. Stanescu-Bellu⁴⁵, M.M. Stanitzki⁴⁵, S. Stapnes¹²¹, E.A. Starchenko¹³²,
 G.H. Stark³³, J. Stark⁵⁸, P. Staroba¹²⁹, P. Starovoitov^{60a}, S. Stärz³², R. Staszewski⁴²,
 P. Steinberg²⁷, B. Stelzer¹⁴⁴, H.J. Stelzer³², O. Stelzer-Chilton^{163a}, H. Stenzel⁵⁵, G.A. Stewart⁵⁶,
 J.A. Stillings²³, M.C. Stockton⁹⁰, M. Stoebe⁹⁰, G. Stoicea^{28b}, P. Stolte⁵⁷, S. Stonjek¹⁰³,
 A.R. Stradling⁸, A. Straessner⁴⁷, M.E. Stramaglia¹⁸, J. Strandberg¹⁴⁹, S. Strandberg^{148a,148b},

A. Strandlie¹²¹, M. Strauss¹¹⁵, P. Strizenec^{146b}, R. Ströhmer¹⁷⁷, D.M. Strom¹¹⁸,
 R. Stroynowski⁴³, A. Strubig¹⁰⁸, S.A. Stucci²⁷, B. Stugu¹⁵, N.A. Styles⁴⁵, D. Su¹⁴⁵, J. Su¹²⁷,
 S. Suchek^{60a}, Y. Sugaya¹²⁰, M. Suk¹³⁰, V.V. Sulin⁹⁸, S. Sultansoy^{4c}, T. Sumida⁷¹, S. Sun⁵⁹,
 X. Sun^{35a}, J.E. Sundermann⁵¹, K. Suruliz¹⁵¹, C.J.E. Suster¹⁵², M.R. Sutton¹⁵¹, S. Suzuki⁶⁹,
 M. Svatos¹²⁹, M. Swiatlowski³³, S.P. Swift², I. Sykora^{146a}, T. Sykora¹³¹, D. Ta⁵¹,
 C. Taccini^{136a,136b}, K. Tackmann⁴⁵, J. Taenzer¹⁶¹, A. Taffard¹⁶⁶, R. Tafirout^{163a}, N. Taiblum¹⁵⁵,
 H. Takai²⁷, R. Takashima⁷², T. Takeshita¹⁴², Y. Takubo⁶⁹, M. Talby⁸⁸, A.A. Talyshv^{111,c},
 K.G. Tan⁹¹, J. Tanaka¹⁵⁷, M. Tanaka¹⁵⁹, R. Tanaka¹¹⁹, S. Tanaka⁶⁹, R. Tanioka⁷⁰,
 B.B. Tannenwald¹¹³, S. Tapia Araya^{34b}, S. Tapprogge⁸⁶, S. Tarem¹⁵⁴, G.F. Tartarelli^{94a},
 P. Tas¹³¹, M. Tasevsky¹²⁹, T. Tashiro⁷¹, E. Tassi^{40a,40b}, A. Tavares Delgado^{128a,128b},
 Y. Tayalati^{137e}, A.C. Taylor¹⁰⁷, G.N. Taylor⁹¹, P.T.E. Taylor⁹¹, W. Taylor^{163b},
 F.A. Teischinger³², P. Teixeira-Dias⁸⁰, K.K. Temming⁵¹, D. Temple¹⁴⁴, H. Ten Kate³²,
 P.K. Teng¹⁵³, J.J. Teoh¹²⁰, F. Tepel¹⁷⁸, S. Terada⁶⁹, K. Terashi¹⁵⁷, J. Terron⁸⁵, S. Terzo¹³,
 M. Testa⁵⁰, R.J. Teuscher^{161,m}, T. Theveneaux-Pelzer⁸⁸, J.P. Thomas¹⁹, J. Thomas-Wilsker⁸⁰,
 P.D. Thompson¹⁹, A.S. Thompson⁵⁶, L.A. Thomsen¹⁷⁹, E. Thomson¹²⁴, M.J. Tibbetts¹⁶,
 R.E. Tice Torres⁸⁸, V.O. Tikhomirov^{98,ap}, Yu.A. Tikhonov^{111,c}, S. Timoshenko¹⁰⁰, P. Tipton¹⁷⁹,
 S. Tisserant⁸⁸, K. Todome¹⁵⁹, T. Todorov^{5,*}, S. Todorova-Nova¹³¹, J. Tojo⁷³, S. Tokár^{146a},
 K. Tokushuku⁶⁹, E. Tolley⁵⁹, L. Tomlinson⁸⁷, M. Tomoto¹⁰⁵, L. Tompkins^{145,aq}, K. Toms¹⁰⁷,
 B. Tong⁵⁹, P. Tornambe⁵¹, E. Torrence¹¹⁸, H. Torres¹⁴⁴, E. Torró Pastor¹⁴⁰, J. Toth^{88,ar},
 F. Touchard⁸⁸, D.R. Tovey¹⁴¹, T. Trefzger¹⁷⁷, A. Tricoli²⁷, I.M. Trigger^{163a}, S. Trincaz-Duvoid⁸³,
 M.F. Tripiana¹³, W. Trischuk¹⁶¹, B. Trocmé⁵⁸, A. Trofymov⁴⁵, C. Troncon^{94a},
 M. Trottier-McDonald¹⁶, M. Trovatelli¹⁷², L. Truong^{167a,167c}, M. Trzebinski⁴², A. Trzupek⁴²,
 J.C-L. Tseng¹²², P.V. Tsiareshka⁹⁵, G. Tsipolitis¹⁰, N. Tsirintanis⁹, S. Tsiskaridze¹³,
 V. Tsiskaridze⁵¹, E.G. Tskhadadze^{54a}, K.M. Tsui^{62a}, I.I. Tsukerman⁹⁹, V. Tsulaia¹⁶, S. Tsuno⁶⁹,
 D. Tsybychev¹⁵⁰, Y. Tu^{62b}, A. Tudorache^{28b}, V. Tudorache^{28b}, T.T. Tulbure^{28a}, A.N. Tuna⁵⁹,
 S.A. Tuppuri^{22a,22b}, S. Turchikhin⁶⁸, D. Turgeman¹⁷⁵, I. Turk Cakir^{4b,as}, R. Turra^{94a,94b},
 P.M. Tuts³⁸, G. Uccielli^{22a,22b}, I. Ueda¹⁵⁷, M. Ughetto^{148a,148b}, F. Ukegawa¹⁶⁴, G. Unal³²,
 A. Undrus²⁷, G. Unel¹⁶⁶, F.C. Ungaro⁹¹, Y. Unno⁶⁹, C. Unverdorben¹⁰², J. Urban^{146b},
 P. Urquijo⁹¹, P. Urrejola⁸⁶, G. Usai⁸, J. Usui⁶⁹, L. Vacavant⁸⁸, V. Vacek¹³⁰, B. Vachon⁹⁰,
 C. Valderanis¹⁰², E. Valdes Santurio^{148a,148b}, N. Valencic¹⁰⁹, S. Valentinetti^{22a,22b}, A. Valero¹⁷⁰,
 L. Valery¹³, S. Valkar¹³¹, J.A. Valls Ferrer¹⁷⁰, W. Van Den Wollenberg¹⁰⁹, P.C. Van Der Deijl¹⁰⁹,
 H. van der Graaf¹⁰⁹, N. van Eldik¹⁵⁴, P. van Gemmeren⁶, J. Van Nieuwkoop¹⁴⁴, I. van Vulpen¹⁰⁹,
 M.C. van Woerden¹⁰⁹, M. Vanadia^{134a,134b}, W. Vandelli³², R. Vanguri¹²⁴, A. Vaniachine¹⁶⁰,
 P. Vankov¹⁰⁹, G. Vardanyan¹⁸⁰, R. Vari^{134a}, E.W. Varnes⁷, T. Varol⁴³, D. Varouchas⁸³,
 A. Vartapetian⁸, K.E. Varvell¹⁵², J.G. Vasquez¹⁷⁹, G.A. Vasquez^{34b}, F. Vazeille³⁷,
 T. Vazquez Schroeder⁹⁰, J. Veatch⁵⁷, V. Veeraraghavan⁷, L.M. Veloce¹⁶¹, F. Veloso^{128a,128c},
 S. Veneziano^{134a}, A. Ventura^{76a,76b}, M. Venturi¹⁷², N. Venturi¹⁶¹, A. Venturini²⁵, V. Vercesi^{123a},
 M. Verducci^{134a,134b}, W. Verkerke¹⁰⁹, J.C. Vermeulen¹⁰⁹, A. Vest^{47,at}, M.C. Vetterli^{144,d},
 O. Viazlo⁸⁴, I. Vichou^{169,*}, T. Vickey¹⁴¹, O.E. Vickey Boeriu¹⁴¹, G.H.A. Viehhauser¹²²,
 S. Viel¹⁶, L. Vigani¹²², M. Villa^{22a,22b}, M. Villaplana Perez^{94a,94b}, E. Vilucchi⁵⁰, M.G. Vinciter³¹,
 V.B. Vinogradov⁶⁸, C. Vittori^{22a,22b}, I. Vivarelli¹⁵¹, S. Vlachos¹⁰, M. Vlasak¹³⁰, M. Vogel¹⁷⁸,
 P. Vokac¹³⁰, G. Volpi^{126a,126b}, M. Volpi⁹¹, H. von der Schmitt¹⁰³, E. von Toerne²³,
 V. Vorobel¹³¹, K. Vorobev¹⁰⁰, M. Vos¹⁷⁰, R. Voss³², J.H. Vosseveld⁷⁷, N. Vranjes¹⁴,
 M. Vranjes Milosavljevic¹⁴, V. Vrba¹²⁹, M. Vreeswijk¹⁰⁹, R. Vuillermet³², I. Vukotic³³,
 P. Wagner²³, W. Wagner¹⁷⁸, H. Wahlberg⁷⁴, S. Wahrmund⁴⁷, J. Wakabayashi¹⁰⁵, J. Walder⁷⁵,
 R. Walker¹⁰², W. Walkowiak¹⁴³, V. Wallangen^{148a,148b}, C. Wang^{35b}, C. Wang^{36b,88}, F. Wang¹⁷⁶,
 H. Wang¹⁶, H. Wang⁴³, J. Wang⁴⁵, J. Wang¹⁵², K. Wang⁹⁰, R. Wang⁶, S.M. Wang¹⁵³,
 T. Wang²³, T. Wang³⁸, W. Wang^{36a}, C. Wanotayaroj¹¹⁸, A. Warburton⁹⁰, C.P. Ward³⁰,

D.R. Wardrope⁸¹, A. Washbrook⁴⁹, P.M. Watkins¹⁹, A.T. Watson¹⁹, M.F. Watson¹⁹, G. Watts¹⁴⁰, S. Watts⁸⁷, B.M. Waugh⁸¹, S. Webb⁸⁶, M.S. Weber¹⁸, S.W. Weber¹⁷⁷, S.A. Weber³¹, J.S. Webster⁶, A.R. Weidberg¹²², B. Weinert⁶⁴, J. Weingarten⁵⁷, C. Weiser⁵¹, H. Weits¹⁰⁹, P.S. Wells³², T. Wenaus²⁷, T. Wengler³², S. Wenig³², N. Wermes²³, M.D. Werner⁶⁷, P. Werner³², M. Wessels^{60a}, J. Wetter¹⁶⁵, K. Whalen¹¹⁸, N.L. Whallon¹⁴⁰, A.M. Wharton⁷⁵, A. White⁸, M.J. White¹, R. White^{34b}, D. Whiteson¹⁶⁶, F.J. Wickens¹³³, W. Wiedenmann¹⁷⁶, M. Wielers¹³³, C. Wiglesworth³⁹, L.A.M. Wiik-Fuchs²³, A. Wildauer¹⁰³, F. Wilk⁸⁷, H.G. Wilkens³², H.H. Williams¹²⁴, S. Williams¹⁰⁹, C. Willis⁹³, S. Willocq⁸⁹, J.A. Wilson¹⁹, I. Wingerter-Seez⁵, F. Winklmeier¹¹⁸, O.J. Winston¹⁵¹, B.T. Winter²³, M. Wittgen¹⁴⁵, T.M.H. Wolf¹⁰⁹, R. Wolff⁸⁸, M.W. Wolter⁴², H. Wolters^{128a,128c}, S.D. Worm¹³³, B.K. Wosiek⁴², J. Wotschack³², M.J. Woudstra⁸⁷, K.W. Wozniak⁴², M. Wu⁵⁸, M. Wu³³, S.L. Wu¹⁷⁶, X. Wu⁵², Y. Wu⁹², T.R. Wyatt⁸⁷, B.M. Wynne⁴⁹, S. Xella³⁹, Z. Xi⁹², D. Xu^{35a}, L. Xu²⁷, B. Yabsley¹⁵², S. Yacoub^{147a}, D. Yamaguchi¹⁵⁹, Y. Yamaguchi¹²⁰, A. Yamamoto⁶⁹, S. Yamamoto¹⁵⁷, T. Yamanaka¹⁵⁷, K. Yamauchi¹⁰⁵, Y. Yamazaki⁷⁰, Z. Yan²⁴, H. Yang^{36c}, H. Yang¹⁷⁶, Y. Yang¹⁵³, Z. Yang¹⁵, W.-M. Yao¹⁶, Y.C. Yap⁸³, Y. Yasu⁶⁹, E. Yatsenko⁵, K.H. Yau Wong²³, J. Ye⁴³, S. Ye²⁷, I. Yeletsikh⁶⁸, E. Yildirim⁸⁶, K. Yorita¹⁷⁴, R. Yoshida⁶, K. Yoshihara¹²⁴, C. Young¹⁴⁵, C.J.S. Young³², S. Youssef²⁴, D.R. Yu¹⁶, J. Yu⁸, J.M. Yu⁹², J. Yu⁶⁷, L. Yuan⁷⁰, S.P.Y. Yuen²³, I. Yusuff^{30,au}, B. Zabinski⁴², R. Zaidan⁶⁶, A.M. Zaitsev^{132,ae}, N. Zakharchuk⁴⁵, J. Zalieckas¹⁵, A. Zaman¹⁵⁰, S. Zambito⁵⁹, L. Zanello^{134a,134b}, D. Zanzi⁹¹, C. Zeitnitz¹⁷⁸, M. Zeman¹³⁰, A. Zemla^{41a}, J.C. Zeng¹⁶⁹, Q. Zeng¹⁴⁵, O. Zenin¹³², T. Ženiš^{146a}, D. Zerwas¹¹⁹, D. Zhang⁹², F. Zhang¹⁷⁶, G. Zhang^{36a,ao}, H. Zhang^{35b}, J. Zhang⁶, L. Zhang⁵¹, L. Zhang^{36a}, M. Zhang¹⁶⁹, R. Zhang²³, R. Zhang^{36a,av}, X. Zhang^{36b}, Z. Zhang¹¹⁹, X. Zhao⁴³, Y. Zhao^{36b,aw}, Z. Zhao^{36a}, A. Zhemchugov⁶⁸, J. Zhong¹²², B. Zhou⁹², C. Zhou¹⁷⁶, L. Zhou³⁸, L. Zhou⁴³, M. Zhou¹⁵⁰, N. Zhou^{35c}, C.G. Zhu^{36b}, H. Zhu^{35a}, J. Zhu⁹², Y. Zhu^{36a}, X. Zhuang^{35a}, K. Zhukov⁹⁸, A. Zibell¹⁷⁷, D. Zieminska⁶⁴, N.I. Zimine⁶⁸, C. Zimmermann⁸⁶, S. Zimmermann⁵¹, Z. Zinonos⁵⁷, M. Zinser⁸⁶, M. Ziolkowski¹⁴³, L. Živković¹⁴, G. Zobernig¹⁷⁶, A. Zoccoli^{22a,22b}, M. zur Nedden¹⁷, L. Zwalinski³²

¹ Department of Physics, University of Adelaide, Adelaide, Australia

² Physics Department, SUNY Albany, Albany NY, United States of America

³ Department of Physics, University of Alberta, Edmonton AB, Canada

⁴ (a) Department of Physics, Ankara University, Ankara; (b) Istanbul Aydın University, Istanbul;

(c) Division of Physics, TOBB University of Economics and Technology, Ankara, Turkey

⁵ LAPP, CNRS/IN2P3 and Université Savoie Mont Blanc, Annecy-le-Vieux, France

⁶ High Energy Physics Division, Argonne National Laboratory, Argonne IL, United States of America

⁷ Department of Physics, University of Arizona, Tucson AZ, United States of America

⁸ Department of Physics, The University of Texas at Arlington, Arlington TX, United States of America

⁹ Physics Department, National and Kapodistrian University of Athens, Athens, Greece

¹⁰ Physics Department, National Technical University of Athens, Zografou, Greece

¹¹ Department of Physics, The University of Texas at Austin, Austin TX, United States of America

¹² Institute of Physics, Azerbaijan Academy of Sciences, Baku, Azerbaijan

¹³ Institut de Física d'Altes Energies (IFAE), The Barcelona Institute of Science and Technology, Barcelona, Spain

¹⁴ Institute of Physics, University of Belgrade, Belgrade, Serbia

¹⁵ Department for Physics and Technology, University of Bergen, Bergen, Norway

¹⁶ Physics Division, Lawrence Berkeley National Laboratory and University of California, Berkeley CA, United States of America

¹⁷ Department of Physics, Humboldt University, Berlin, Germany

¹⁸ Albert Einstein Center for Fundamental Physics and Laboratory for High Energy Physics, University of Bern, Bern, Switzerland

- ¹⁹ *School of Physics and Astronomy, University of Birmingham, Birmingham, United Kingdom*
- ²⁰ ^(a) *Department of Physics, Bogazici University, Istanbul;* ^(b) *Department of Physics Engineering, Gaziantep University, Gaziantep;* ^(d) *Istanbul Bilgi University, Faculty of Engineering and Natural Sciences, Istanbul, Turkey;* ^(e) *Bahcesehir University, Faculty of Engineering and Natural Sciences, Istanbul, Turkey, Turkey*
- ²¹ *Centro de Investigaciones, Universidad Antonio Narino, Bogota, Colombia*
- ²² ^(a) *INFN Sezione di Bologna;* ^(b) *Dipartimento di Fisica e Astronomia, Università di Bologna, Bologna, Italy*
- ²³ *Physikalisches Institut, University of Bonn, Bonn, Germany*
- ²⁴ *Department of Physics, Boston University, Boston MA, United States of America*
- ²⁵ *Department of Physics, Brandeis University, Waltham MA, United States of America*
- ²⁶ ^(a) *Universidade Federal do Rio De Janeiro COPPE/EE/IF, Rio de Janeiro;* ^(b) *Electrical Circuits Department, Federal University of Juiz de Fora (UFJF), Juiz de Fora;* ^(c) *Federal University of Sao Joao del Rei (UFSJ), Sao Joao del Rei;* ^(d) *Instituto de Fisica, Universidade de Sao Paulo, Sao Paulo, Brazil*
- ²⁷ *Physics Department, Brookhaven National Laboratory, Upton NY, United States of America*
- ²⁸ ^(a) *Transilvania University of Brasov, Brasov, Romania;* ^(b) *Horia Hulubei National Institute of Physics and Nuclear Engineering, Bucharest;* ^(c) *National Institute for Research and Development of Isotopic and Molecular Technologies, Physics Department, Cluj Napoca;* ^(d) *University Politehnica Bucharest, Bucharest;* ^(e) *West University in Timisoara, Timisoara, Romania*
- ²⁹ *Departamento de Física, Universidad de Buenos Aires, Buenos Aires, Argentina*
- ³⁰ *Cavendish Laboratory, University of Cambridge, Cambridge, United Kingdom*
- ³¹ *Department of Physics, Carleton University, Ottawa ON, Canada*
- ³² *CERN, Geneva, Switzerland*
- ³³ *Enrico Fermi Institute, University of Chicago, Chicago IL, United States of America*
- ³⁴ ^(a) *Departamento de Física, Pontificia Universidad Católica de Chile, Santiago;* ^(b) *Departamento de Física, Universidad Técnica Federico Santa María, Valparaíso, Chile*
- ³⁵ ^(a) *Institute of High Energy Physics, Chinese Academy of Sciences, Beijing;* ^(b) *Department of Physics, Nanjing University, Jiangsu;* ^(c) *Physics Department, Tsinghua University, Beijing 100084, China*
- ³⁶ ^(a) *Department of Modern Physics, University of Science and Technology of China, Anhui;* ^(b) *School of Physics, Shandong University, Shandong;* ^(c) *Department of Physics and Astronomy, Shanghai Key Laboratory for Particle Physics and Cosmology, Shanghai Jiao Tong University, Shanghai; (also affiliated with PKU-CHEP), China*
- ³⁷ *Laboratoire de Physique Corpusculaire, Université Clermont Auvergne, Université Blaise Pascal, CNRS/IN2P3, Clermont-Ferrand, France*
- ³⁸ *Nevis Laboratory, Columbia University, Irvington NY, United States of America*
- ³⁹ *Niels Bohr Institute, University of Copenhagen, Kobenhavn, Denmark*
- ⁴⁰ ^(a) *INFN Gruppo Collegato di Cosenza, Laboratori Nazionali di Frascati;* ^(b) *Dipartimento di Fisica, Università della Calabria, Rende, Italy*
- ⁴¹ ^(a) *AGH University of Science and Technology, Faculty of Physics and Applied Computer Science, Krakow;* ^(b) *Marian Smoluchowski Institute of Physics, Jagiellonian University, Krakow, Poland*
- ⁴² *Institute of Nuclear Physics Polish Academy of Sciences, Krakow, Poland*
- ⁴³ *Physics Department, Southern Methodist University, Dallas TX, United States of America*
- ⁴⁴ *Physics Department, University of Texas at Dallas, Richardson TX, United States of America*
- ⁴⁵ *DESY, Hamburg and Zeuthen, Germany*
- ⁴⁶ *Lehrstuhl für Experimentelle Physik IV, Technische Universität Dortmund, Dortmund, Germany*
- ⁴⁷ *Institut für Kern- und Teilchenphysik, Technische Universität Dresden, Dresden, Germany*
- ⁴⁸ *Department of Physics, Duke University, Durham NC, United States of America*
- ⁴⁹ *SUPA - School of Physics and Astronomy, University of Edinburgh, Edinburgh, United Kingdom*
- ⁵⁰ *INFN Laboratori Nazionali di Frascati, Frascati, Italy*
- ⁵¹ *Fakultät für Mathematik und Physik, Albert-Ludwigs-Universität, Freiburg, Germany*

- 52 *Departement de Physique Nucleaire et Corpusculaire, Université de Genève, Geneva, Switzerland*
- 53 ^(a) *INFN Sezione di Genova;* ^(b) *Dipartimento di Fisica, Università di Genova, Genova, Italy*
- 54 ^(a) *E. Andronikashvili Institute of Physics, Iv. Javakishvili Tbilisi State University, Tbilisi;* ^(b) *High Energy Physics Institute, Tbilisi State University, Tbilisi, Georgia*
- 55 *II Physikalisches Institut, Justus-Liebig-Universität Giessen, Giessen, Germany*
- 56 *SUPA - School of Physics and Astronomy, University of Glasgow, Glasgow, United Kingdom*
- 57 *II Physikalisches Institut, Georg-August-Universität, Göttingen, Germany*
- 58 *Laboratoire de Physique Subatomique et de Cosmologie, Université Grenoble-Alpes, CNRS/IN2P3, Grenoble, France*
- 59 *Laboratory for Particle Physics and Cosmology, Harvard University, Cambridge MA, United States of America*
- 60 ^(a) *Kirchhoff-Institut für Physik, Ruprecht-Karls-Universität Heidelberg, Heidelberg;* ^(b) *Physikalisches Institut, Ruprecht-Karls-Universität Heidelberg, Heidelberg;* ^(c) *ZITI Institut für technische Informatik, Ruprecht-Karls-Universität Heidelberg, Mannheim, Germany*
- 61 *Faculty of Applied Information Science, Hiroshima Institute of Technology, Hiroshima, Japan*
- 62 ^(a) *Department of Physics, The Chinese University of Hong Kong, Shatin, N.T., Hong Kong;* ^(b) *Department of Physics, The University of Hong Kong, Hong Kong;* ^(c) *Department of Physics and Institute for Advanced Study, The Hong Kong University of Science and Technology, Clear Water Bay, Kowloon, Hong Kong, China*
- 63 *Department of Physics, National Tsing Hua University, Taiwan, Taiwan*
- 64 *Department of Physics, Indiana University, Bloomington IN, United States of America*
- 65 *Institut für Astro- und Teilchenphysik, Leopold-Franzens-Universität, Innsbruck, Austria*
- 66 *University of Iowa, Iowa City IA, United States of America*
- 67 *Department of Physics and Astronomy, Iowa State University, Ames IA, United States of America*
- 68 *Joint Institute for Nuclear Research, JINR Dubna, Dubna, Russia*
- 69 *KEK, High Energy Accelerator Research Organization, Tsukuba, Japan*
- 70 *Graduate School of Science, Kobe University, Kobe, Japan*
- 71 *Faculty of Science, Kyoto University, Kyoto, Japan*
- 72 *Kyoto University of Education, Kyoto, Japan*
- 73 *Department of Physics, Kyushu University, Fukuoka, Japan*
- 74 *Instituto de Física La Plata, Universidad Nacional de La Plata and CONICET, La Plata, Argentina*
- 75 *Physics Department, Lancaster University, Lancaster, United Kingdom*
- 76 ^(a) *INFN Sezione di Lecce;* ^(b) *Dipartimento di Matematica e Fisica, Università del Salento, Lecce, Italy*
- 77 *Oliver Lodge Laboratory, University of Liverpool, Liverpool, United Kingdom*
- 78 *Department of Experimental Particle Physics, Jožef Stefan Institute and Department of Physics, University of Ljubljana, Ljubljana, Slovenia*
- 79 *School of Physics and Astronomy, Queen Mary University of London, London, United Kingdom*
- 80 *Department of Physics, Royal Holloway University of London, Surrey, United Kingdom*
- 81 *Department of Physics and Astronomy, University College London, London, United Kingdom*
- 82 *Louisiana Tech University, Ruston LA, United States of America*
- 83 *Laboratoire de Physique Nucléaire et de Hautes Energies, UPMC and Université Paris-Diderot and CNRS/IN2P3, Paris, France*
- 84 *Fysiska institutionen, Lunds universitet, Lund, Sweden*
- 85 *Departamento de Física Teórica C-15, Universidad Autónoma de Madrid, Madrid, Spain*
- 86 *Institut für Physik, Universität Mainz, Mainz, Germany*
- 87 *School of Physics and Astronomy, University of Manchester, Manchester, United Kingdom*
- 88 *CPPM, Aix-Marseille Université and CNRS/IN2P3, Marseille, France*
- 89 *Department of Physics, University of Massachusetts, Amherst MA, United States of America*
- 90 *Department of Physics, McGill University, Montreal QC, Canada*
- 91 *School of Physics, University of Melbourne, Victoria, Australia*
- 92 *Department of Physics, The University of Michigan, Ann Arbor MI, United States of America*

- ⁹³ *Department of Physics and Astronomy, Michigan State University, East Lansing MI, United States of America*
- ⁹⁴ ^(a) *INFN Sezione di Milano;* ^(b) *Dipartimento di Fisica, Università di Milano, Milano, Italy*
- ⁹⁵ *B.I. Stepanov Institute of Physics, National Academy of Sciences of Belarus, Minsk, Republic of Belarus*
- ⁹⁶ *Research Institute for Nuclear Problems of Byelorussian State University, Minsk, Republic of Belarus*
- ⁹⁷ *Group of Particle Physics, University of Montreal, Montreal QC, Canada*
- ⁹⁸ *P.N. Lebedev Physical Institute of the Russian Academy of Sciences, Moscow, Russia*
- ⁹⁹ *Institute for Theoretical and Experimental Physics (ITEP), Moscow, Russia*
- ¹⁰⁰ *National Research Nuclear University MEPhI, Moscow, Russia*
- ¹⁰¹ *D.V. Skobel'syn Institute of Nuclear Physics, M.V. Lomonosov Moscow State University, Moscow, Russia*
- ¹⁰² *Fakultät für Physik, Ludwig-Maximilians-Universität München, München, Germany*
- ¹⁰³ *Max-Planck-Institut für Physik (Werner-Heisenberg-Institut), München, Germany*
- ¹⁰⁴ *Nagasaki Institute of Applied Science, Nagasaki, Japan*
- ¹⁰⁵ *Graduate School of Science and Kobayashi-Maskawa Institute, Nagoya University, Nagoya, Japan*
- ¹⁰⁶ ^(a) *INFN Sezione di Napoli;* ^(b) *Dipartimento di Fisica, Università di Napoli, Napoli, Italy*
- ¹⁰⁷ *Department of Physics and Astronomy, University of New Mexico, Albuquerque NM, United States of America*
- ¹⁰⁸ *Institute for Mathematics, Astrophysics and Particle Physics, Radboud University Nijmegen/Nikhef, Nijmegen, Netherlands*
- ¹⁰⁹ *Nikhef National Institute for Subatomic Physics and University of Amsterdam, Amsterdam, Netherlands*
- ¹¹⁰ *Department of Physics, Northern Illinois University, DeKalb IL, United States of America*
- ¹¹¹ *Budker Institute of Nuclear Physics, SB RAS, Novosibirsk, Russia*
- ¹¹² *Department of Physics, New York University, New York NY, United States of America*
- ¹¹³ *Ohio State University, Columbus OH, United States of America*
- ¹¹⁴ *Faculty of Science, Okayama University, Okayama, Japan*
- ¹¹⁵ *Homer L. Dodge Department of Physics and Astronomy, University of Oklahoma, Norman OK, United States of America*
- ¹¹⁶ *Department of Physics, Oklahoma State University, Stillwater OK, United States of America*
- ¹¹⁷ *Palacký University, RCPTM, Olomouc, Czech Republic*
- ¹¹⁸ *Center for High Energy Physics, University of Oregon, Eugene OR, United States of America*
- ¹¹⁹ *LAL, Univ. Paris-Sud, CNRS/IN2P3, Université Paris-Saclay, Orsay, France*
- ¹²⁰ *Graduate School of Science, Osaka University, Osaka, Japan*
- ¹²¹ *Department of Physics, University of Oslo, Oslo, Norway*
- ¹²² *Department of Physics, Oxford University, Oxford, United Kingdom*
- ¹²³ ^(a) *INFN Sezione di Pavia;* ^(b) *Dipartimento di Fisica, Università di Pavia, Pavia, Italy*
- ¹²⁴ *Department of Physics, University of Pennsylvania, Philadelphia PA, United States of America*
- ¹²⁵ *National Research Centre "Kurchatov Institute" B.P.Konstantinov Petersburg Nuclear Physics Institute, St. Petersburg, Russia*
- ¹²⁶ ^(a) *INFN Sezione di Pisa;* ^(b) *Dipartimento di Fisica E. Fermi, Università di Pisa, Pisa, Italy*
- ¹²⁷ *Department of Physics and Astronomy, University of Pittsburgh, Pittsburgh PA, United States of America*
- ¹²⁸ ^(a) *Laboratório de Instrumentação e Física Experimental de Partículas - LIP, Lisboa;* ^(b) *Faculdade de Ciências, Universidade de Lisboa, Lisboa;* ^(c) *Department of Physics, University of Coimbra, Coimbra;* ^(d) *Centro de Física Nuclear da Universidade de Lisboa, Lisboa;* ^(e) *Departamento de Física, Universidade do Minho, Braga;* ^(f) *Departamento de Física Teórica y del Cosmos and CAFPE, Universidad de Granada, Granada (Spain);* ^(g) *Dep Física and CEFITEC of Faculdade de Ciências e Tecnologia, Universidade Nova de Lisboa, Caparica, Portugal*
- ¹²⁹ *Institute of Physics, Academy of Sciences of the Czech Republic, Praha, Czech Republic*

- 130 *Czech Technical University in Prague, Praha, Czech Republic*
- 131 *Faculty of Mathematics and Physics, Charles University in Prague, Praha, Czech Republic*
- 132 *State Research Center Institute for High Energy Physics (Protvino), NRC KI, Russia*
- 133 *Particle Physics Department, Rutherford Appleton Laboratory, Didcot, United Kingdom*
- 134 ^(a) *INFN Sezione di Roma;* ^(b) *Dipartimento di Fisica, Sapienza Università di Roma, Roma, Italy*
- 135 ^(a) *INFN Sezione di Roma Tor Vergata;* ^(b) *Dipartimento di Fisica, Università di Roma Tor Vergata, Roma, Italy*
- 136 ^(a) *INFN Sezione di Roma Tre;* ^(b) *Dipartimento di Matematica e Fisica, Università Roma Tre, Roma, Italy*
- 137 ^(a) *Faculté des Sciences Ain Chock, Réseau Universitaire de Physique des Hautes Energies - Université Hassan II, Casablanca;* ^(b) *Centre National de l'Energie des Sciences Techniques Nucleaires, Rabat;* ^(c) *Faculté des Sciences Semlalia, Université Cadi Ayyad, LPHEA-Marrakech;* ^(d) *Faculté des Sciences, Université Mohamed Premier and LPTPM, Oujda;* ^(e) *Faculté des sciences, Université Mohammed V, Rabat, Morocco*
- 138 *DSM/IRFU (Institut de Recherches sur les Lois Fondamentales de l'Univers), CEA Saclay (Commissariat à l'Energie Atomique et aux Energies Alternatives), Gif-sur-Yvette, France*
- 139 *Santa Cruz Institute for Particle Physics, University of California Santa Cruz, Santa Cruz CA, United States of America*
- 140 *Department of Physics, University of Washington, Seattle WA, United States of America*
- 141 *Department of Physics and Astronomy, University of Sheffield, Sheffield, United Kingdom*
- 142 *Department of Physics, Shinshu University, Nagano, Japan*
- 143 *Fachbereich Physik, Universität Siegen, Siegen, Germany*
- 144 *Department of Physics, Simon Fraser University, Burnaby BC, Canada*
- 145 *SLAC National Accelerator Laboratory, Stanford CA, United States of America*
- 146 ^(a) *Faculty of Mathematics, Physics & Informatics, Comenius University, Bratislava;* ^(b) *Department of Subnuclear Physics, Institute of Experimental Physics of the Slovak Academy of Sciences, Kosice, Slovak Republic*
- 147 ^(a) *Department of Physics, University of Cape Town, Cape Town;* ^(b) *Department of Physics, University of Johannesburg, Johannesburg;* ^(c) *School of Physics, University of the Witwatersrand, Johannesburg, South Africa*
- 148 ^(a) *Department of Physics, Stockholm University;* ^(b) *The Oskar Klein Centre, Stockholm, Sweden*
- 149 *Physics Department, Royal Institute of Technology, Stockholm, Sweden*
- 150 *Departments of Physics & Astronomy and Chemistry, Stony Brook University, Stony Brook NY, United States of America*
- 151 *Department of Physics and Astronomy, University of Sussex, Brighton, United Kingdom*
- 152 *School of Physics, University of Sydney, Sydney, Australia*
- 153 *Institute of Physics, Academia Sinica, Taipei, Taiwan*
- 154 *Department of Physics, Technion: Israel Institute of Technology, Haifa, Israel*
- 155 *Raymond and Beverly Sackler School of Physics and Astronomy, Tel Aviv University, Tel Aviv, Israel*
- 156 *Department of Physics, Aristotle University of Thessaloniki, Thessaloniki, Greece*
- 157 *International Center for Elementary Particle Physics and Department of Physics, The University of Tokyo, Tokyo, Japan*
- 158 *Graduate School of Science and Technology, Tokyo Metropolitan University, Tokyo, Japan*
- 159 *Department of Physics, Tokyo Institute of Technology, Tokyo, Japan*
- 160 *Tomsk State University, Tomsk, Russia, Russia*
- 161 *Department of Physics, University of Toronto, Toronto ON, Canada*
- 162 ^(a) *INFN-TIFPA;* ^(b) *University of Trento, Trento, Italy, Italy*
- 163 ^(a) *TRIUMF, Vancouver BC;* ^(b) *Department of Physics and Astronomy, York University, Toronto ON, Canada*
- 164 *Faculty of Pure and Applied Sciences, and Center for Integrated Research in Fundamental Science and Engineering, University of Tsukuba, Tsukuba, Japan*

- 165 *Department of Physics and Astronomy, Tufts University, Medford MA, United States of America*
- 166 *Department of Physics and Astronomy, University of California Irvine, Irvine CA, United States of America*
- 167 ^(a) *INFN Gruppo Collegato di Udine, Sezione di Trieste, Udine;* ^(b) *ICTP, Trieste;* ^(c) *Dipartimento di Chimica, Fisica e Ambiente, Università di Udine, Udine, Italy*
- 168 *Department of Physics and Astronomy, University of Uppsala, Uppsala, Sweden*
- 169 *Department of Physics, University of Illinois, Urbana IL, United States of America*
- 170 *Instituto de Física Corpuscular (IFIC) and Departamento de Física Atómica, Molecular y Nuclear and Departamento de Ingeniería Electrónica and Instituto de Microelectrónica de Barcelona (IMB-CNM), University of Valencia and CSIC, Valencia, Spain*
- 171 *Department of Physics, University of British Columbia, Vancouver BC, Canada*
- 172 *Department of Physics and Astronomy, University of Victoria, Victoria BC, Canada*
- 173 *Department of Physics, University of Warwick, Coventry, United Kingdom*
- 174 *Waseda University, Tokyo, Japan*
- 175 *Department of Particle Physics, The Weizmann Institute of Science, Rehovot, Israel*
- 176 *Department of Physics, University of Wisconsin, Madison WI, United States of America*
- 177 *Fakultät für Physik und Astronomie, Julius-Maximilians-Universität, Würzburg, Germany*
- 178 *Fakultät für Mathematik und Naturwissenschaften, Fachgruppe Physik, Bergische Universität Wuppertal, Wuppertal, Germany*
- 179 *Department of Physics, Yale University, New Haven CT, United States of America*
- 180 *Yerevan Physics Institute, Yerevan, Armenia*
- 181 *Centre de Calcul de l'Institut National de Physique Nucléaire et de Physique des Particules (IN2P3), Villeurbanne, France*
- ^a *Also at Department of Physics, King's College London, London, United Kingdom*
- ^b *Also at Institute of Physics, Azerbaijan Academy of Sciences, Baku, Azerbaijan*
- ^c *Also at Novosibirsk State University, Novosibirsk, Russia*
- ^d *Also at TRIUMF, Vancouver BC, Canada*
- ^e *Also at Department of Physics & Astronomy, University of Louisville, Louisville, KY, United States of America*
- ^f *Also at Physics Department, An-Najah National University, Nablus, Palestine*
- ^g *Also at Department of Physics, California State University, Fresno CA, United States of America*
- ^h *Also at Department of Physics, University of Fribourg, Fribourg, Switzerland*
- ⁱ *Also at Departament de Física de la Universitat Autònoma de Barcelona, Barcelona, Spain*
- ^j *Also at Departamento de Física e Astronomia, Faculdade de Ciências, Universidade do Porto, Portugal*
- ^k *Also at Tomsk State University, Tomsk, Russia, Russia*
- ^l *Also at Università di Napoli Parthenope, Napoli, Italy*
- ^m *Also at Institute of Particle Physics (IPP), Canada*
- ⁿ *Also at Horia Hulubei National Institute of Physics and Nuclear Engineering, Bucharest, Romania*
- ^o *Also at Department of Physics, St. Petersburg State Polytechnical University, St. Petersburg, Russia*
- ^p *Also at Department of Physics, The University of Michigan, Ann Arbor MI, United States of America*
- ^q *Also at Centre for High Performance Computing, CSIR Campus, Rosebank, Cape Town, South Africa*
- ^r *Also at Louisiana Tech University, Ruston LA, United States of America*
- ^s *Also at Institutio Catalana de Recerca i Estudis Avancats, ICREA, Barcelona, Spain*
- ^t *Also at Graduate School of Science, Osaka University, Osaka, Japan*
- ^u *Also at Institute for Mathematics, Astrophysics and Particle Physics, Radboud University Nijmegen/Nikhef, Nijmegen, Netherlands*
- ^v *Also at Department of Physics, The University of Texas at Austin, Austin TX, United States of America*

- ^w Also at Institute of Theoretical Physics, Iia State University, Tbilisi, Georgia
- ^x Also at CERN, Geneva, Switzerland
- ^y Also at Georgian Technical University (GTU), Tbilisi, Georgia
- ^z Also at O Chadai Academic Production, Ochanomizu University, Tokyo, Japan
- ^{aa} Also at Manhattan College, New York NY, United States of America
- ^{ab} Also at Academia Sinica Grid Computing, Institute of Physics, Academia Sinica, Taipei, Taiwan
- ^{ac} Also at School of Physics, Shandong University, Shandong, China
- ^{ad} Also at Department of Physics, California State University, Sacramento CA, United States of America
- ^{ae} Also at Moscow Institute of Physics and Technology State University, Dolgoprudny, Russia
- ^{af} Also at Departement de Physique Nucleaire et Corpusculaire, Université de Genève, Geneva, Switzerland
- ^{ag} Also at Eotvos Lorand University, Budapest, Hungary
- ^{ah} Also at Departments of Physics & Astronomy and Chemistry, Stony Brook University, Stony Brook NY, United States of America
- ^{ai} Also at International School for Advanced Studies (SISSA), Trieste, Italy
- ^{aj} Also at Department of Physics and Astronomy, University of South Carolina, Columbia SC, United States of America
- ^{ak} Also at Institut de Física d'Altes Energies (IFAE), The Barcelona Institute of Science and Technology, Barcelona, Spain
- ^{al} Also at School of Physics, Sun Yat-sen University, Guangzhou, China
- ^{am} Also at Institute for Nuclear Research and Nuclear Energy (INRNE) of the Bulgarian Academy of Sciences, Sofia, Bulgaria
- ^{an} Also at Faculty of Physics, M.V.Lomonosov Moscow State University, Moscow, Russia
- ^{ao} Also at Institute of Physics, Academia Sinica, Taipei, Taiwan
- ^{ap} Also at National Research Nuclear University MEPhI, Moscow, Russia
- ^{aq} Also at Department of Physics, Stanford University, Stanford CA, United States of America
- ^{ar} Also at Institute for Particle and Nuclear Physics, Wigner Research Centre for Physics, Budapest, Hungary
- ^{as} Also at Giresun University, Faculty of Engineering, Turkey
- ^{at} Also at Flensburg University of Applied Sciences, Flensburg, Germany
- ^{au} Also at University of Malaya, Department of Physics, Kuala Lumpur, Malaysia
- ^{av} Also at CPPM, Aix-Marseille Université and CNRS/IN2P3, Marseille, France
- ^{aw} Also at LAL, Univ. Paris-Sud, CNRS/IN2P3, Université Paris-Saclay, Orsay, France
- * Deceased